Biomechanical Regulation of Arteriogenesis: Defining Critical Endothelial-dependent Events

by

Peter J. Mack

S.M. Mechanical Engineering
Massachusetts Institute of Technology, 2004

B.S. Mechanical Engineering
University of Notre Dame, 2002

SUBMITTED TO THE DIVISION OF HEALTH SCIENCES AND TECHNOLOGY IN PARTIAL FULFILLMENT OF THE REQUIREMENTS FOR THE DEGREE OF

DOCTOR OF PHILOSOPHY IN MEDICAL ENGINEERING
AT THE
MASSACHUSETTS INSTITUTE OF TECHNOLOGY

AUGUST 2008

Signature of Author: _____
Division of Health Sciences and Technology
August 11, 2008

Certified by: _____
Guillermo García-Cardeña, Ph.D.
Assistant Professor of Pathology
Harvard Medical School
Thesis Supervisor

Certified by: _____
Roger D. Kamm, Ph.D.
Germeshausen Professor of Mechanical and Biological Engineering
Associated Head, Mechanical Engineering
Thesis Chair and Supervisor

Accepted by: _____
Martha L. Gray, Ph.D.
Edward Hood Taplin Professor of Medical and Electrical Engineering
Director, Harvard-MIT Division of Health Sciences and Technology

Abstract

Coronary heart disease (CHD) is a major health concern for Americans and people worldwide. Arteriogenesis, an adaptive remodeling process in which pre-existing collateral arterioles remodel to form large diameter conductance arteries, has received recent attention for its therapeutic potential in treating CHD, but the mechanisms regulating the process remain incompletely understood. In particular, little is known about how collateral flow, and the resulting effect of shear stress acting along the collateral vessel wall, regulates coronary collateralization. This Thesis combines a series of experimental systems to define the responses evoked in endothelial cells exposed to hemodynamic waveforms characteristic of coronary collateral vessels and the subsequent paracrine effects on smooth muscle cells.

Initially, a lumped parameter model of the human coronary collateral circulation was used to simulate normal (NCC) and adaptive remodeling (ACC) coronary collateral shear stress waveforms. These waveforms were then applied to cultured human endothelial cells (EC) and the resulting differences in EC gene expression were assessed by genome-wide transcriptional profiling, identifying genes distinctly regulated by collateral flow, including genes important for endothelial-smooth muscle interactions. In particular, the transcription factor KLF2 was upregulated by the ACC waveform and several of its downstream targets displayed the expected modulation, including the downregulation of Connective tissue growth factor (CTGF). Moreover, delivery of endothelial conditioned medium generated throughout the collateral flow experiments to culture smooth muscle cells (SMC) resulted in the modulation of SMC genes related to vessel maturation and stabilization. In the second part of this Thesis, the effect of endothelial KLF2 expression on SMC migration was characterized using a 3D microfluidic assay capable of monitoring SMC migration in co-culture with EC. Using this 3D system, it was found that KLF2-expressing EC co-cultured with SMC significantly reduce SMC migration compared to control EC and that this reduction can be rescued by delivery of soluble CTGF. Collectively, these results demonstrate that the shear stress generated by collateral flow evokes distinct EC gene expression profiles and functional phenotypes that subsequently influence vascular events important for adaptive remodeling and provides experimental evidence supporting efforts directed at investigating endothelial KLF2 as a molecular target for therapeutic arteriogenesis.

Thesis Supervisor:

Guillermo García-Cardeña, Ph.D.

Assistant Professor of Pathology

Brigham and Women's Hospital and Harvard Medical School

Thesis Chair and Supervisor:

Roger D. Kamm, Ph.D.

Germeshausen Professor of Mechanical and Biological Engineering

Associate Head, Mechanical Engineering

Massachusetts Institute of Technology

Thesis Committee Members:

Rakesh Jain, Ph.D.

Andrew Werk Cook Professor of Tumor Biology

Department of Radiation Oncology

Massachusetts General Hospital and Harvard Medical School

Richard T. Lee, M.D.

Associate Professor of Medicine

Brigham and Women's Hospital and Harvard Medical School

Table of Contents

Figures list

Chapter 1: Background

1.1 Coronary heart disease

Coronary heart disease (CHD) is a significant health concern in America and it is estimated that each year 700,000 Americans will have a new coronary event while 500,000 will have a recurrent one (1). The pathophysiology of CHD involves progressive, focal atherosclerotic plaque development and narrowing and/or complete occlusion of the blood vessel lumen. Since the main function of the coronary arteries is to perfuse myocardial tissue, clinical consequences of CHD include chronic or intermittent ischemia, presenting as angina, and myocardial infarction. As the diagnostic tools and therapeutic approaches for detecting CHD have evolved, the number of people receiving bypass grafts or implantable stents has continued to increase (1). However, a subset of patients with advanced disease do not qualify for these treatments based on the number or size of the occluded vessel(s), while other patients develop restenosis at the site of repair that requires further surgical intervention (2). It is now recognized that reperfusion of ischemic myocardial regions can occur biologically through coronary collateralization/arteriogenesis – a process where pre-existing collateral arterioles undergo adaptive remodeling to form large diameter conductance arteries which bypass a site of arterial occlusion (Figure 1.1). Therapeutic arteriogenesis provides a promising avenue of intervention

in the treatment of CHD, but current clinical efforts have afforded little success, creating the need to better understand the physiological mechanisms by which these unique vessels develop, remodel and mature into arteries capable of providing sufficient perfusion to prevent distal tissue ischemia. A number of open questions exist in the field of arteriogenesis ranging from understanding the basic biological mechanisms to establishing efficacious therapeutics. It is generally accepted, however, that collateral vessel hemodynamics provides a significant stimulus for adaptive arteriogenesis and that the endothelium is required for both acute and chronic vascular remodeling. Furthermore, correlative data exist indicating an inverse relationship between age and diabetes-induced endothelial dysfunction and coronary collateralization (3). Taken together, these observations relating local hemodynamics, endothelial function, and the clinical potential of therapeutic arteriogenesis provide the motivational basis to explore mechanistically the process of arteriogenesis and in particular how biomechanical forces distinct to coronary collaterals influence the functional phenotype of vascular cells.

1.2 Vascular remodeling and adaptive arteriogenesis

Cells of the blood vessel wall interact through an intricate intercellular signaling pattern in response to their surrounding environment. Endothelial cells, which line the blood vessel lumen, and smooth muscle cells, which comprise the structural layers of the vessel wall, respond to changes in the local hemodynamic environment by producing and responding to autocrine and paracrine mediators that can ultimately influence blood vessel formation, tone, and remodeling. Adaptive remodeling is one such process that involves the modulation of several endothelial and

smooth muscle functions, as well as alterations to the surrounding extracellular matrix (4,5). Moreover, this process is dependent upon a dynamic interaction between locally generated growth factors and cytokines, vasoactive substances, and biomechanical stimuli. The vessel wall can acutely dilate or constrict with changes in hemodynamics and over time the structure of the vessel reorganizes in order to preserve arterial flow, as described by Glagov's phenomenon (6). As a result, reorganization of the vessel wall depends on the stimuli imposed. General inward remodeling or reduction in the vessel lumen can result from reduced blood flow where as expansive remodeling occurs over time under conditions of increased flow. Thus, chronic arterial adaptation and remodeling reflect the summation of both short-term vasomotor events as well as long-term functional and structural adaptations. The importance of the endothelium in adaptive vascular responses has been established by the seminal observations that endothelial cell denudation prevents arterial remodeling in response to acute and chronic hemodynamic changes and, furthermore, endothelial-derived factors have been shown to be required for vascular remodeling (7-9).

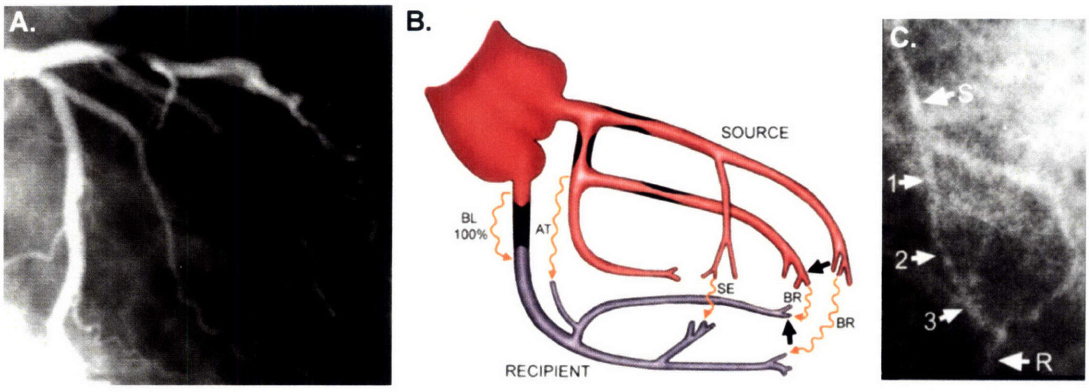

Figure 1.1 Adaptive arteriogenesis or coronary collateralization occurs in the clinical context of coronary artery disease. (A) 2D magnetic resonance angiographic assessment of coronary artery stenosis. (B) Collateral vessels develop into four main types: Bridging across lesion (BL), branch-branch ventricular free wall (BR), atrial (AT), and septal (SE). (C) Developed collateral vessels can be seen by angiography where the source vessel (S) bypasses a site of coronary stenosis in order to perfuse a recipient vessel (R). Here a single BL collateral vessel is shown and marked at three separate locations by 1,2, and 3 (10).

Coronary collateralization or arteriogenesis, a specific type of adaptive remodeling, occurs in the context of arterial occlusion when pre-existing collateral arterioles remodel to form larger diameter bypass arteries. The current arteriogenesis paradigm implicates local hemodynamics, recruitment/activation of monocytes, and structural remodeling of the vascular wall as key steps in collateralization (5). Two primary stages of collateralization have been described based predominantly on observations from femoral artery ligation models that induce collateral modeling via an instantaneous increase in collateral flow. The initial stage of collateralization is characterized by a wave of monocyte-driven inflammation and rapid vasodilation, an immediate compensatory response to the increased collateral flow. In the second phase of collateralization, the initial inflammatory response is resolved and the newly formed conductance artery matures and the wall stabilizes to accommodate the increase in blood conductance (9). Collectively, these relatively rapid changes in the local vessel environment collectively result in matrix remodeling, vessel enlargement and stabilization via the recruitment, differentiation, and proliferation of vascular cells (4). To-date considerable attention has been dedicated to investigating the inflammatory regulation of this process (i.e. MCP-1 and GM-CSF), but despite evidence on the importance of the endothelium and endothelial-derived factors in flow-mediated arterial remodeling, less is known about the particular effect altered collateral flow has on the endothelium and the resulting regulation of downstream adaptive remodeling processes (7-9). Therefore, characterizing the role collateral flow, or more specifically the shear stress pattern resulting from collateral flow, plays in regulating the functional endothelial cell phenotype and endothelial-dependent processes associated with adaptive remodeling, including paracrine affects on smooth muscle cells, should provide a framework to better understand the establishment, maintenance, and remodeling of arteries.

Unlike angiogenesis and vasculogenesis in which new vessel development is driven by tissue hypoxia, adaptive arteriogenesis occurs in response to alterations in biomechanical force and local inflammatory activity within pre-existing collateral arterioles near the site of arterial occlusion. Arterial remodeling is known to occur in the context of both healthy and diseased arteries. Healthy arteries respond to acute changes in hemodynamic flow and hormonal stimulation with rapid vasodilation or vasoconstriction, as well as to chronic changes in blood flow and pressure in an effort of maintain shear stress and vessel wall stability. For example, endothelial nitric oxide (NO) production regulates acute vasodilation by signaling to smooth muscle cells for relaxation in response to elevated fluid shear stress (11) and longer-term vessel maturation as an important cue to perivascular cells (12), while chronic hypertension leads to smooth muscle cell-mediated remodeling of connective tissue (13). Conversely, smooth muscle cell proliferation associated with intimal hyperplasia and inward remodeling occurs in response to inflammatory cell stimulation during atherosclerosis and restenosis, as well as conditions of lowered blood flow (14). Although these pathological remodeling processes share a number of characteristics with the initial stage of adaptive arteriogenesis, particularly increased inflammatory cell activity and smooth muscle proliferation, the inflammation associated with adaptive arteriogenesis resolves within a relatively short period of time (on the order of days) after which smooth muscle cells of the vascular wall acquire a differentiated contractile phenotype and the newly formed artery stabilizes (15). Furthermore, it remains unclear how collateral flow acting on the endothelium throughout the stages of collateral formation distinguishes arteriogenesis from pathological vascular remodeling.

A number of signaling molecules have been identified and characterized, using both *in vitro* endothelial-smooth muscle co-culture assays and *in vivo* animal models, as pro-arteriogenic

for their role in endothelial-smooth muscle cell interactions during arteriogenesis and vessel maturation. Animal models of embryogenesis using knock-out mice have elucidated both endothelial and perivascular cell-specific genes necessary for arteriogenesis and the development of mature vessels, many of which observe a lethal impairment of perivascular cell incorporation or function within the developing blood vessels (Figure 1.2, adapted from Carmeliet, 2003) (16). Furthermore, a number of endothelial-specific knock-out mice display embryonic lethality with vascular wall defects including Kruppel-like factor 2 (KLF2), Platelet-derived growth factor B (PDGF-BB), Angiopoietin-1, and Sphingosine-1 phosphate-1 (S1P1), suggesting a critical role for endothelial signaling to smooth muscle cells, while embryonic lethal perivascular knock-out genes include Platelet-derived growth factor receptor B (PDGFRB) and Endoglin, a receptor for Transforming growth factor beta (TGF-β) (12,17,18). Furthermore, knock-out mice lacking the macrophage receptor for Monocyte chemotactic protein-1 (MCP-1) show impaired collateral vessel growth in adult mice following experimental arterial occlusion (4).

In vitro endothelial-smooth muscle cell, or smooth muscle precursor cell (10T1/2 cell line), co-culture and conditioned medium assays support a number of the knock-out mice findings. Notably, TGF-β and S1P1 have been shown to be critical for smooth muscle precursor cell differentiation towards an adult smooth muscle cell based on the expression of alpha-Smooth muscle actin (αSMA), while endothelial-derived PDGF-BB and MCP-1 have both been shown to stimulate smooth muscle precursor migration (19-21). Smooth muscle Kruppel-like factors 4 and 5 (KLF4 and KLF5) are increasingly being acknowledged for their role in dictating these changes in smooth muscle cell phenotype. In particular, KLF4 competes at the promoter level with the smooth muscle transcriptional co-activator Myocardin to suppress the expression contractile smooth muscle markers (22), such as αSMA, while the expression of KLF5 has

recently been documented in proliferating smooth muscle cells in response to injury and during vascular remodeling (23). Although the *in vitro* conditioned medium and endothelial-smooth muscle precursor co-culture assays show consistent observations with knowledge gained from knock-out mice studies of vessel maturation, they lacked the capability to investigate the isolated effects of physiological shear stress acting on the endothelium in these endothelial-smooth muscle cell interactions.

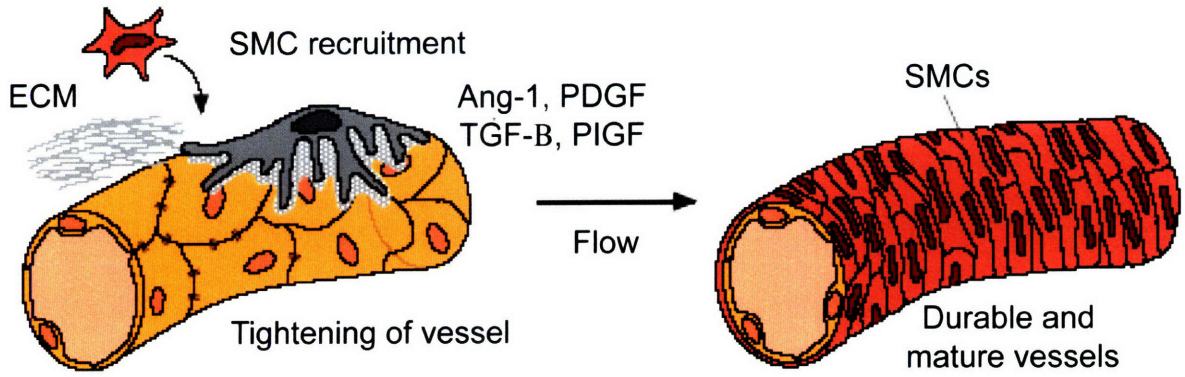

Figure 1.2 During development, blood vessels form first as a nascent endothelial tube and later perivascular cells are recruited to the vessel wall. These nascent vessels mature into larger diameter vessels characteristic of the arterial circulation that have a wall containing differentiated smooth muscle cells (SMC). The transition from a nascent to mature vessel depends on the hemodynamic forces generated by flow within these vessels, as well paracrine factors generated by the endothelium that signal to the surrounding smooth muscle cells. Although the process of vessel maturation is best described in the embryo, aspects of the biological process may hold true during post-natal vascular remodeling and specifically for the case of coronary collateralization or adaptive arteriogenesis (adapted from Carmeliet, 2003) (16).

The relevance of specific signaling molecules towards arteriogenesis, including GM-CSF, MCP-1, and basic Fibroblastic growth factor (bFGF), have primarily been demonstrated using models in which an instantaneous total occlusion of the femoral artery is surgically created

in the hind limb of an animal (24). The effect of the occlusion and signaling molecules on collateral remodeling and distal ischemia-driven angiogenesis is then assessed using Doppler flow measurements and tissue histology. These hind limb models have revealed fundamental characteristics and mechanisms of adaptive arteriogenesis, but are limited in their ability to investigate the specific role shear stress has on influencing endothelial-derived paracrine signals acting on smooth muscle cells that are critical for arteriogenesis. More recently, the hind limb model has been adapted by creating an arterial-venous shunt distal to the site of occlusion in order to increase the collateral vessel pressure difference and generate greater collateral flow. The additional increase in flow along collateral arterioles in this adapted model result in elevated endothelial expression of inflammatory adhesion (VCAM-1 and ICAM-1) and signaling (GM-CSF, MCP-1) molecules (25), as well as greater inflammatory cell infiltration. However, in addition to creating a non-physiological change in pressure along collateral vessels, it is unclear if the inflammatory activation of the endothelium with the modified hind limb model is an isolated effect of the elevation in shear stress or an integrated effect of all the environmental changes local to the site of occlusion. Thus, based on our incomplete understanding of the endothelial response during arteriogenesis, a clear need exists to better understand the direct effect of shear stress acting along the collateral endothelium and its impact on adaptive arteriogenesis.

1.3 Endothelial mechanotransduction

The premise for investigating the role of biomechanical forces in arteriogenesis is rooted in the concept of mechanotransduction – a process by which cells transduce mechanical forces into

biological responses. Mechanotransdution occurs across a variety of time and length scales, influencing single molecule events, cellular signals, tissue morphogenesis, and organ function in both acute and chronic settings. Initial cellular-level investigations into the role of mechanical forces in regulating biological functions often focused on stretch-activated ion channels, particularly in hair cells. More recently, mechnotransduction has been systematically investigated as the tools for applying defined forces and measuring biological read-outs have advanced. Investigations of mechanotransduction have revealed molecular-level interactions ubiquitous to a variety of cells and tissues, such as the effect of force on structural protein binding (26), as well as tissue-specific phenomenon for bone (27), cartilage (28), the myocardium (29), and the endothelium (30).

The vascular endothelium is constantly exposed to hemodynamic forces and it has been determined that the tangential component of this biomechanical stimulus, or shear stress, is a major determinant of endothelial phenotypes (31-33). Initiating mechanisms of shear-induced endothelial mechanotransduction likely involve the activation of ion channels, G protein coupled receptors or other transmembrane receptors, and forced-induced conformational changes to cytoskeletal and focal adhesion proteins (34), but emerging evidence also suggests that other cellular components (e.g. primary cilia and the glycocalyx on the apical surface of endothelial cells) can also affect the cellular response to external force (35,36). Regardless of the precise physical basis for endothelial mechanotransduction, the downstream effect of mechanical signal transduction leads to changes in endothelial gene expression, molecular phenotype, and function. The response of single endothelial cells and a confluent endothelial monolayer of cells to external force depends on the magnitude, duration, and temporal variation of force (37,38). Translated into vascular pathophysiology, this indicates that the endothelium can differentiate

between shear stress waveforms present in distinct locations within the human vasculature in both physiologic and pathophysiologic states. One well established example of this phenomenon is the effect of arterial shear stress patterns on evoking endothelial phenotypes critical for protection against atherosclerosis. In particular, waveforms present at branch points within the arterial vasculature show disturbed flow patterns and the forces imposed on the endothelium by this type of flow contributes to endothelial dysfunction, whereas waveforms derived from regions protected against atherogenesis evoke anti-inflammatory, anti-thrombotic, and vasoactive endothelial phenotypes (39,40). Furthermore, given both acute and chronic flow-mediated vascular remodeling depends on the presence of an intact endothelium, endothelial mechanotransduction is most likely critical for vascular remodeling as well (7).

1.4 Kruppel-like factor 2 (KLF2)

Under pathophysiological conditions, endothelial interactions with circulating cells and humoral factors can initiate and sustain immune responses and thrombotic events during both acute and chronic disease states. Normal, healthy endothelium, however, possesses several molecular checkpoints to prevent its dysfunction, and the subsequent development of vascular pathologies. This "vasoprotective" endothelial functional phenotype has been shown to be dependent in large part on the particular type of hemodynamic environments present in the vessel wall. The vasoprotective action of biomechanical force acting on the endothelium has been primarily focused on the effects of hemodynamic shear stress, and multiple studies have documented mechano-activated signaling pathways, and specific patterns of gene expression are associated

with endothelial vasoprotection. The transcription factor Kruppel-like factor 2 (KLF2) has recently been shown to be a key integrator of the flow-mediated endothelial vasoprotective phenotype and its expression *in vivo* and in culture is intimately linked to the pattern and magnitude of shear stress acting on the endothelium (40,41). In particular, atheroprotective shear stress waveforms derived from regions within the human internal carotid artery protected against the development of atherosclerosis result in significant upregulation of KLF2 expression and suppression of pro-inflammatory and thrombogenic activity compared to endothelial cells exposed to static (no shear stress) or shear stress waveforms derived from atherosclerosis-susceptible regions of the human carotid sinus. Moreover, these observations have singled out KLF2 as an attractive therapeutic target for the prevention and treatment of cardiovascular disease (42), and highlight the importance of identifying new regulators of KLF2 as modifiers of endothelial vasoprotection. However, it remains to be determined whether KLF2 expression in the endothelium plays a critical role in adaptive vascular remodeling processes, such as coronary collateralization.

Kruppel-like factors (KLFs) are a subclass of the zinc-finger family of transcription factors that contain a similar DNA binding domain. KLFs typically bind to GC-rich or CACCC sequences in the promoter region of target genes to regulate transcriptional activity. In contrast to the zinc-finger regions, the non-DNA-binding regions are highly divergent and modular activation and repression domains have been identified that regulate transcriptional activity (43). The nomenclature is based on homology to the DNA-binding domain of the Drosophila protein Kruppel. Since the identification of EKLF/KLF1, a number of experimental approaches ranging from homology screening to bioinformatics have been employed to identify additional Kruppel-like factors. To date, 17 mammalian KLFs have been identified and are designated KLF1

through KLF17, based on the chronologic sequence of identification. KLF2, a member of this zinc finger family of transcription factors, is primarily found in osteoclasts, T-cells, and endothelial cells of adult tissue (23). Embryonic stem cells also express KLF2 and this transcription factor has been identified as one of the interchangeable Kruppels required for embryonic stem cell self-renewal (44).

Evidence from *in vivo* models indicates that the transcription factor may have a critical role in adaptive remodeling since mice lacking KLF2 display lethal phenotypes of impaired vascular maturation and function. Both *KLF2* -/- mice and endothelial-specific knockout of KLF2 in mice result in embryonic lethality, due either to hemorrhage (17,45) or defects in vascular hemodynamics (46), respectively. Moreover, a recent report by Wu, J et al. documented that the medial layer of vessels of *KLF2*-/- mice is poorly developed, and that SMC of these mice display a patchy morphology with condensed nuclei when compared to wild-type mice (47). None of these mouse models, however, displayed impaired vasculogenic capacity, implying that the principal vascular defect associated with KLF2 loss involves ineffective regulation, potentially via the endothelium, of smooth muscle functions associated with vessel wall stability and reactivity.

1.5 Thesis approach and goals

Based on the evidence linking altered flow to adaptive arteriogenesis, combined with knowledge surrounding endothelial mechanosensing and the molecular basis for endothelial-smooth muscle cell interactions during arterial formation, it is reasonable to hypothesize that hemodynamic shear stress acting on collateral vessel endothelium following arterial occlusion stimulates the

endothelial cells to promote arteriogenesis through the control of vascular smooth muscle cell events critical for arterial remodeling, including gene expression, migration, and proliferation (Figure 1.3). To experimentally address this hypothesis a series of interrelated steps were taken. First, in Chapter 2, the fluid shear stress waveforms characteristic collateral vessel blood flow during arterial occlusion was numerically simulated using a lumped parameter mode. Next, in Chapter 3, these shear stress waveforms were applied to cultured human endothelial cells and the resulting differences in endothelial cell gene expression were assessed by genome-wide transcriptional profiling to identify genes distinctly regulated by collateral flow. Analysis of these transcriptional programs identified several genes to be differentially regulated by collateral flow, including genes important for endothelial-smooth muscle interactions. Also in Chapter 3, the functional significance of collateral flow acting on the endothelium was evaluated by delivering collateral flow-mediated paracrine signals from the endothelium to cultured smooth muscle cells and assessing for differences in smooth muscle gene expression. Lastly, in Chapter 4, molecular regulation of endothelial-induced smooth muscle recruitment, a critical smooth muscle cell phenotype associated with vessel stabilization and maturation during arteriogenesis, was explored based on information gained from the collateral flow-mediated endothelial transcriptional profiles.

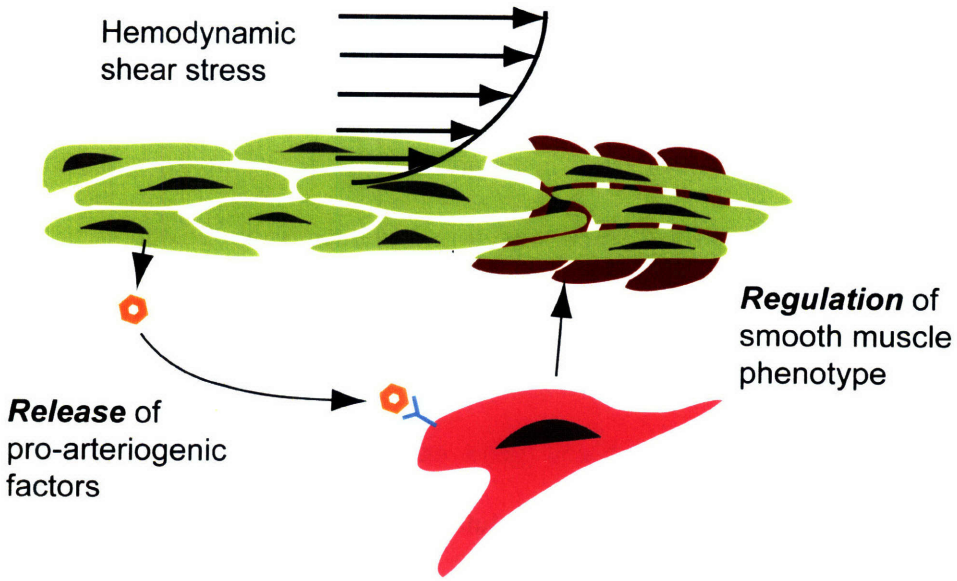

Figure 1.3 Schematic of how hemodynamic shear stress or collateral flow acting on the endothelium may regulate cellular events critical for arteriogenesis, including the generation of pro-arteriogenic paracrine factors within the endothelium and their regulation of smooth muscle phenotypes.

Three primary experimental systems were employed in order to study interactions between endothelial and smooth muscle cells important for arteriogenesis. None of the co-culture systems used here allowed direct contact between endothelial and smooth muscle cells and thus selectively investigated the specific effect of endothelial paracrine signals on regulating smooth muscle phenotypes. The first experimental system combines a cone-and-plate shear device, capable of applying defined shear stress waveforms to cultured endothelial cells, with a smooth muscle cell culture chamber in order to characterize the effect flow-mediated endothelial paracrine signals, via conditioned medium, have on smooth muscle cell gene expression and proliferation. Mass transport from the endothelial compartment to the smooth muscle compartment is on the order of minutes so the paracrine factors of interest with this system primarily have long bioactivity, such as growth factors. The second experimental system, on the

other hand, permits the transport of labile factors by co-culturing endothelial and smooth muscle cells on opposite sides of a 10 μm transwell porous membrane. The endothelium, though grown under static conditions, can be genetically manipulated to investigate the effect of specific endothelial genes on regulating smooth muscle gene expression and proliferation. Finally, a microfluidic device was used to generate a three dimensional smooth muscle migration assay where smooth muscle cell migration was monitored in response to endothelial-derived factors. The endothelium can be genetically manipulated in this system to explore the molecular mechanisms of endothelial-smooth muscle cell interactions, similar to the transwell system, but this system has the unique advantage of supporting more physiological cell growth with its three dimensional environment.

By coupling these experimental systems, each capable of mimicking specific aspects of endothelial-smooth muscle cell interactions relevant to coronary collateralization, it was possible to address fundamental mechanistic questions surrounding arteriogenesis. In particular, the experimental systems employed here have the distinct advantage of applying well characterized collateral shear stress patterns to endothelial cells, while eliminating local inflammatory activity and isolating the pro-arteriogenic effect of hemodynamic shear stress on the endothelium. Furthermore, the role of specific endothelial genes in regulating smooth muscle interactions was investigated using multiple controlled environments.

The ultimate goal of Thesis was to identify mechano-activated endothelial paracrine signals critical for controlling smooth muscle cell phenotypic changes relevant to arteriogenesis and adaptive vascular remodeling. In addressing this goal, two main themes emerged: First, collateral flow evokes vascular cell phenotypes consistent with blood vessel maturation and stability, two states critical for the long-term maintenance of large diameter conductance arteries;

and second, endothelial paracrine signals dependent the transcription factor KLF2 collectively act to restrict smooth muscle cell migration, a functional event important for the maintenance of a normal arterial wall architecture. Taken together, the contributions from this Thesis has expanded the knowledge regarding biomechanical control of arteriogenesis, which has broader applications in understanding blood vessel maturation and arterial formation, and may ultimately impact clinical approaches aimed at stimulating therapeutic arteriogenesis in the context of coronary heart disease.

Chapter 2: Numerical Characterization of Coronary Collateral Waveforms

2.1 Introduction

Elevation in collateral vessel blood flow is a hallmark of adaptive arteriogenesis and even though significant knowledge exists relating endothelial mechanotransduction to both acute and chronic vascular remodeling, there is little evidence connecting fluid shear stress with specific endothelial responses in the context of arteriogenesis. By definition, coronary collateralization is the adult remodeling, initiated by coronary occlusion, of pre-existing arterioles or resistance vessels into arterial conductance vessels (Figure 1.1). Based on the hypothesis that the collateral vessel flow associated with a clinically significant coronary occlusion evokes pro-arteriogenic endothelial phenotypes, a series of interrelated experiments have been pursued that depended on obtaining physiological representations of the shear stress waveforms acting along collateral vessel endothelium in both normal and diseased conditions. A number of strategies for simulating the pressure-flow rate relationship for various vessels in cardiovascular hemodynamics been used by others, but none have specifically sought to characterize the coronary collateral circulation. Importantly, the precedent has been set for applying numerical estimates of the pulsatile shear stress waveforms from distinct locations within the human vasculature to cultured endothelial cells in order to elucidate important molecular mechanisms of

vascular health and disease (39). The main approaches to numerically simulating cardiovascular hemodynamics include local analysis (i.e. finite element analysis) and systemic analysis (i.e. lumped parameter analysis). Finite element analysis of blood flow is a powerful tool for investigating the local hemodynamics of vessel segments and branch points, capable of taking into account vessel geometry and fluid-solid interactions with sub-millimeter resolution (39,48-50). Alternatively, lumped parameter models of both the peripheral (51) and coronary circulation (52), in which vessel segments are assigned hemodynamic equivalent elements of an electrical circuit, have been used to characterize bulk pressure-flow rate relationships that accurately predict flow rates and pressures consistent with experimentally obtained data.

With the goal of simulating blood flow and the shear stress waveforms through the coronary collateral vessels during normal coronary collateral flow (designated NCC), in the absence of coronary artery disease, and during arteriogenic coronary collateral flow (designated ACC), in the presence of a clinically significant coronary artery occlusion that shunts blood flow to the collaterals, a lumped parameter approach was chosen (Figure 2.1 and Figure 2.2). Although theoretically capable of generating detailed local fluid dynamic analysis of collateral vessels, finite element analysis was deemed infeasible for such a model due to significant variability between individual collaterals and limitations in obtaining high resolution measurements of the detailed collateral geometry (coronary angiography is currently limited to a resolution of 200 μm) and local time-varying flow rate necessary to generate a finite element model. Thus, this chapter outlines the assumptions made in generating the lumped parameter model of the coronary collateral circulation and in conducting the numerical simulations and discusses the results and significance of the simulated waveforms in the context of adaptive arteriogenesis. Overall, the resulting coronary collateral waveforms constitute the first known

numerical estimates of the shear stress patterns present in normal and arteriogenic coronary collaterals and should provide the biomechanical foundation to experimentally investigate the role of biomechanical forces in coronary collateralization.

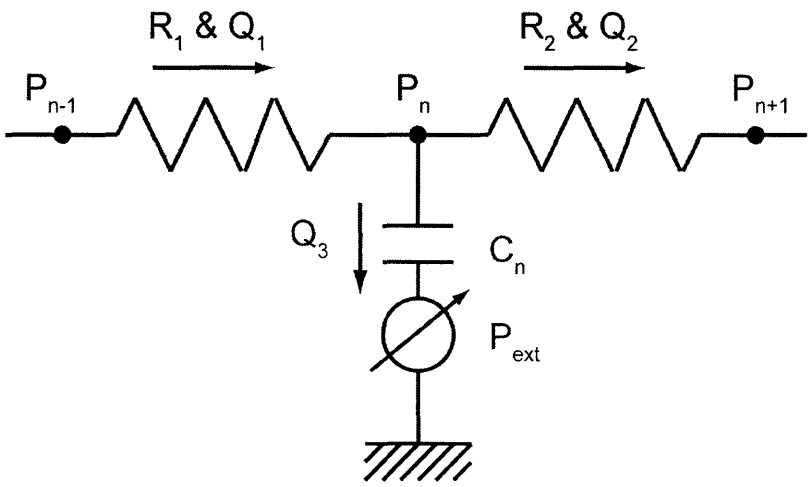

Figure 2.1 Lumped-parameter simulations of cardiovascular hemodynamics model cardiovascular parameters with electrical circuit equivalents. A generalized lumped parameter element is defined by the upstream and downstream pressure (P) and resistance (R), as well as the vessel compliance (C) and external pressure (P_{ext}). With these parameters, the vascular segment can be used to solve for the nodal pressure (P_n) using the relationship between flow rate (Q) and resistance ($Q = \Delta P/R$) along with Kirchoff's law for conservation of mass (Q1 = Q2 + Q3).

2.2 Methods

2.2.1 Coronary collateral model assumptions

A number of assumptions for the lumped parameter model were made based on what is currently known regarding the geometric parameters influencing the coronary collateral circulation. The assumptions relate to the pre-existing collateral path, geometric dimensions, and abundance. First, four types of collateral vessels have previously been defined based on the location of

collateral initiation: septal (SE), atrial (AT), branch-branch in ventricular free walls (BR), and bridging across lesions (BL) (Figure 1.1B). The model used here assumes a bridging across lesion (BL) geometry in which coronary collateral vessels originate from the same artery containing an occlusion and terminate distal to the occlusion (Figure 2.2). Based on one clinical study, this is a common collateral geometry was observed in 12 out of 52 patients with severe coronary stenosis (10). Accordingly, the lumped parameter electrical circuit equivalent for this collateral path is a collateral vessel segment in parallel with the stenotic portion of coronary artery (Figure 2.2). The remaining segments of the coronary circulation are then assembled in series either upstream or downstream of the collateral as dictated by the appropriate anatomy. Next, the collateral size and distribution (i.e. number of collateral vessels bypassing a stenosis), two characteristics known to vary significantly between patients as well as between individual stenosis in a single patient, were estimated. Although histological evaluation of the myocardial tissue surrounding a site of coronary stenosis may provide clues as to the relative distribution of these collateral vessel characteristics, the stage of collateral remodeling would be largely unknown. Collateral vessels that exist prior to coronary occlusion are defined as resistance vessels, but over time and in the presence of coronary occlusion these vessels remodel with an expanding diameter. The vessels of interest for this simulation are pre-developed collaterals at the onset of arteriogenesis, which have the size scale of resistance vessels (arterioles or small arteries) and thus cannot be accurately imaged in the human heart. Typically, it is only after the collateral vessels have developed into conductance arteries that they can be visualized with angiography. Studies characterizing the geometry of fully developed conductance collateral vessels found these vessels range in diameter from 300 μm – 1.4 mm (10). Since the goal of the present simulation is to estimate collateral vessel hemodynamics at the onset of collateral

remodeling (i.e. first and second stage) and not following their development into conductance vessels, a collateral vessel diameter of 200 μm, below the limit for angiography, was assumed. Similarly, it is difficult to accurately predict the number of collateral vessels that surround a site of coronary occlusion based on variability between samples and limitations in the measurement technique. It has been proposed that 1-100 pre-existing collaterals may bypass a single site of stenosis and, for the purposes of this simulation, 10 collateral vessels in parallel and of equal diameter were assumed to bypass the site of occlusion. However, for the no stenosis (NCC) and partial stenosis (ACC) simulations, the number of collateral vessels, ranging from 1 to 100, does not significantly influence the outcome of the simulation because the pressure difference along the vessel segment is predominately determined by the resistance across the stenotic vessel. Lastly, a degree of coronary stenosis must be assigned to the model for the case of partial stenosis (ACC). Clinically, a coronary stenosis greater than 50% is considered a significant risk for myocardial infarction and more than 90% of patients with a coronary artery occlusion greater than or equal to 70% experience angina (53). Thus, in order to maintain clinical relevance while generating hemodynamic shear stress values that are both feasible to reproduce *in vitro* and are on the order of arterial shear stress values, a concentric coronary artery stenosis of 60% radius (85% area) reduction was assumed.

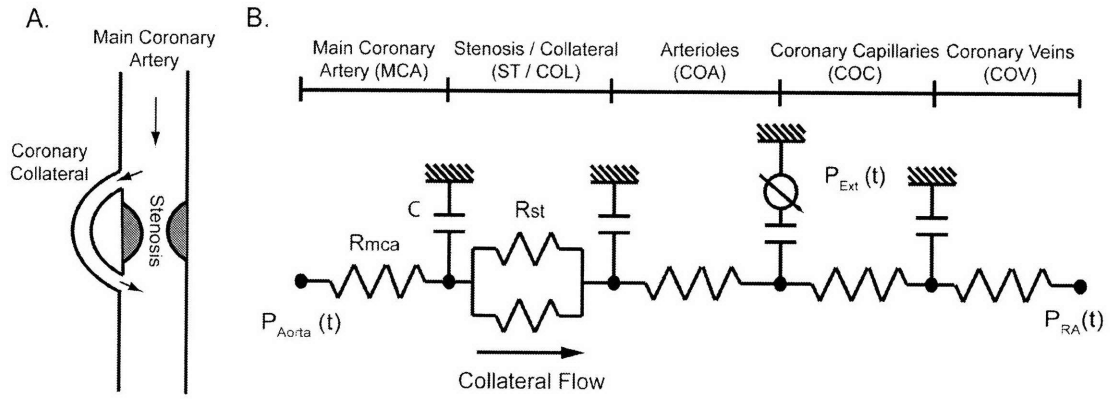

Figure 2.2 Numerical simulation of human coronary collateral hemodynamics. A) Schematic of bridging-type collateral vessel bypassing a site of coronary stenosis. B) A lumped parameter model of the coronary circulation, inclusive of coronary collaterals in parallel with a site of coronary stenosis, was used to simulate the shear stress waveforms present in collateral vessels. The model assigns electrical circuit equivalents to each vascular segment (i.e. vascular resistance, R, and compliance, C) and uses the appropriate pressure, P(t), boundary conditions to solve for the pressure difference across each segment, which was then used to obtain the time-varying wall shear stress acting along each segment. Time-varying pressure tracing boundary conditions for the aorta (P_{Aorta}), right atrium (P_{RA}), and left ventricle ($P_{ext} = 0.75xP_{lv}$) were obtained from Heldt et al, 2002.

2.2.3 Numerical solution to collateral model

The electrical circuit equivalents in lumped parameter hemodynamic models include resistance R as vascular resistance that is expressed in peripheral vascular resistance units (1 PRU = 1 mmHg·s/ml), voltage as hydrodynamic pressure P (mmHg), current as flow rate Q (ml/s), and capacitance as vascular compliance C (ml/mmHg). Modeling a single vascular element required an inflow (R_1) and an outflow (R_2) resistance, vessel compliance C_n, and an external (biased) pressure P_{ext} (Figure 2.1). In order to solve for the node pressure P_n, conservation of mass at node "n" must be satisfied and the two known boundary pressures (P_{n-1} and P_{n+1}) must be specified. Applying Kirchoff's law to each node of the lumped parameter model yielded the following equation for conservation of mass:

$$\frac{dV}{dt} = Q_3 = Q_1 - Q_2 \qquad (1)$$

where flow rate Q is related to the pressure drop ΔP across a resistance element R by,

$$Q = \Delta P / R \tag{2}$$

and the instantaneous volume V at each node is related to the external pressure $P_{ext}(t)$ and the vessel compliance C by,

$$V = C \times (P_n - P_{ext}(t)). \tag{3}$$

Substituting Eqn2 into Eqn1 for Q_1 and Q_2 while substituting the time derivative of Eqn3 into Eqn1 yielded a differential equation for pressure that can be solved at node "n" if the boundary pressures are specified.

The differential equation characterizing a single vessel segment was then be expanded to model multiple interconnected vascular segments. Here, the coronary circulation was modeled with the following segments: main coronary artery (mca), stenotic artery (st) in parallel with a variable number of collateral vessels (col) with equal resistance, coronary arteriole (coa), coronary capillary (coc), and coronary vein (cov) (Figure 2.2B). Solving for conservation of mass at each node in this coronary circulation model produced a series of differential equations which can be solved with the following matrix:

$$d\vec{P} / dt = A\vec{P} + \vec{b} \tag{4}$$

where P is a vector containing the nodal pressures, A is a hemodynamic exchange constant that depends on the segment resistance and compliance, and b is a vector containing the system input values. For the simulations, a system of ordinary differential equations for the coronary circulation was developed using Eqn4 and solved using the fourth order Runga-Kutta method in Matlab. The time varying boundary values for aortic pressure P_{ao} and right atrial pressure P_{ra} were obtained from previously published data (Figure 2.3) (51).

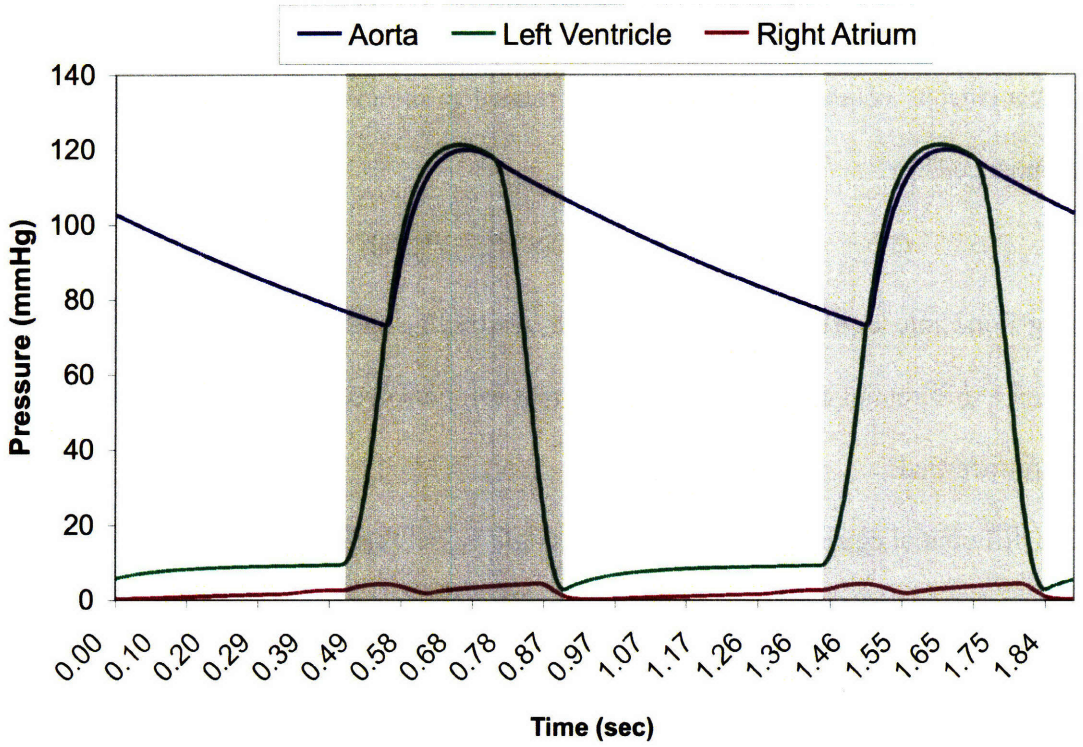

Figure 2.3 The pressure boundary conditions required to solve the lumped parameter model of the coronary collateral circulation were obtained from previously published data (51) for the Aorta (Ao), Left Ventricle (LV), and Right Atrium (RA). The shaded regions correspond to systole.

Depending on the pressure difference across each vessel segment, conservation of mass at each node can take on either a "forward flow" or a "reverse flow" relationship (details for individual nodes can be found in the Appendix). The solution for Eqn4 yielded time-varying nodal pressures tracings, which were then used to calculate the instantaneous pressure difference across each vessel segment, ΔP, for both the normal (NCC) and arteriogenic (ACC) coronary collateral simulations, and subsequently the wall shear stress τ acting along the collateral vessel by:

$$\tau = \frac{r\Delta P}{2L} \tag{5}$$

where r is the vessel radius, L is the vessel length, and ΔP is the pressure difference across the specific segment.

Parameter designation for vessel resistance and compliance was obtained from previously published data where available or estimated using the appropriate fluid dynamic principles (see Table 2.1 for details). Specific considerations were also made for the volume dependent nature of capillary and venous resistance by applying an inverse quadratic relationship in which the instantaneous resistance R_i is calculated from the reference resistance R_o, the instantaneous volume V, and the constant $\beta = 1$ mmHg·s·ml for dimensional consistency:

$$R_i = R_o + \left(\beta / V^2\right) \tag{6}$$

where the capillary volume V_{coc} is found by

$$V_{coc} = (P_{coc} - P_{ext}(t)) \times C_{coc} \tag{7}$$

and the venous volume is found by

$$V_{cov} = P_{cov} \times C_{cov}. \tag{8}$$

Vascular Bed	Resistance (PRU)	Compliance (ml/mmHg)
Main coronary artery (mca)	0.044*	0.003
Arterioles (coa)	27	0.003
Capillaries (coc)	2.7	0.4
Veins (cov)	0.6	0.25
Collateral (col)	5730*	
Stenosis (st)		
NCC	0.044*	
ACC	0.2-0.5*	

Table 2.1 Coronary collateral circulation lumped parameter designation for vascular segment electrical circuit equivalents (resistance and compliance) were obtained from previously published data (52) or fluid dynamic estimates, as denoted by *.

Previous lumped parameter simulations of the coronary circulation have found that in order to obtain realistic pressure-flow rate relationships, the external pressure associated with myocardial contraction during systole must also be accounted for at the level of the capillaries. This effect was achieved by applying a time-varying external pressure $P_{cxt}(t)$ to the capillary node, as can be seen in Figure 6 and Eqn7. Experimental data has shown that this external pressure is roughly 75% of the left ventricular pressure P_{lv} (52). Thus, for the purposes of these simulations

$$P_{ext}(t) = 0.75 \times P_{lv}(t) \tag{9}$$

where $P_{lv}(t)$ is obtained from previously published data (51).

Collateral vessel and main coronary artery resistances were estimated assuming fully developed, steady, laminar Poiseuille flow:

$$R_i = \frac{\Delta P}{Q} = \frac{8\pi\mu L}{A^2} \tag{10}$$

where A is the vessel cross-sectional area, L is the vessel length, and μ is the viscosity of blood (μ = 0.003 Pa·s). Using an upper bound collateral vessel diameter of D = 200 μm and length L = 1 cm for the collateral vessel dimensions yielded a resistance R_{col} of 5730 PRU while using D = 0.5 cm and L = 3 cm yielded a main coronary artery resistance R_{mca} of 0.044 PRU. Although the resistance through the main coronary artery is negligible in comparison to the resistance through the entire coronary system, a relative value for the vessel resistance was required in order to estimate the resistance through the stenosis, which was modeled for two cases: (i) a "no stenosis" or normal coronary collateral (NCC) case in which the stenosis resistance R_{st} equals the main coronary artery (R_{st} = R_{mca} = 0.044 PRU) and (ii) a "partial stenosis" or arteriogenic coronary collateral (ACC) case in which the stenosis resistance was considered nonlinear due to the exit expansion and estimated from conservation of momentum. The case of "total occlusion" in which R_{st} = 100,000 was also used, but the values of shear stress obtained exceed physiologic levels and what is possible to reproduce experimentally by multiple orders of magnitude. Finally, the nonlinear "partial stenosis" resistance was estimated by applying conservation of linear momentum,

$$\frac{d}{dt}\iiint_V \rho U dV + \iint_A \rho U(U \cdot n)dA = \iint_A -(p \cdot n)dA + \iint_S \tau dS + \iiint_V \rho g dV \qquad (11)$$

Assuming negligible contributions from acceleration, wall shear stress, and gravity, a time-varying non-linear form of the stenosis resistance R_{st} was estimated by balancing momentum flux with the pressure contribution, resulting in:

$$R_{st} = \frac{\Delta p}{Q_{st}} = \rho Q_{st}\left(\frac{(A_1 - A_2)^2}{2A_1^2 A_2^2}\right) \qquad (12)$$

where the resistance of the stenosis becomes a function of the cross-sectional area for the stenosis A_1 and the normal vessel A_2, the blood density ρ (1060 kg/m^3), and the instantaneous flow rate Q_{st} through the stenosis.

2.3 Results

The lumped parameter model was solved for two hemodynamically distinct collateral vessels: First, the normal coronary collateral (designated NCC), in which there is no stenosis in the upstream main coronary artery and, second, the arteriogenic coronary collateral (designated ACC), in which there is a 60% radius reduction of the upstream main coronary artery exists (Figure 2.4). To calculate the corresponding collateral waveforms, the time-varying nodal pressures for these vessels were first solved for with the coronary collateral lumped parameter model by assigning previously published or fluid dynamically estimated parameters (i.e. vascular resistance, R, and compliance, C) to each vessel segment of the and applying the pressure tracing, $P_i(t)$, boundary conditions, as described in detail in the Methods section. Once obtaining the time-varying pressure tracing at each node, the shear stress waveforms were calculated by substituting the change in pressure across the collateral vessel, which equaled the instantaneous pressure difference between the main coronary artery and the coronary arterioles ($P_{mca} - P_{coa}$), into Eqn5. The solution yielded two distinct pulsatile shear stress waveforms with the arteriogenic coronary collateral (ACC) waveform having an arterial level of shear stress and the normal coronary collateral (NCC) waveform being approximately one order of magnitude less (Figure 2.4). For these simulated waveforms, the degree of main coronary artery stenosis, numerically the resistance through the vessel segment in parallel with the collateral vessel, was

the major determinant of the simulated collateral shear stress magnitude. The number of collateral vessels, ranging from 1 to 100, did not significantly affect the waveform, and the collateral vessel diameter, which could also significantly affect the waveform magnitude, was held constant for the two simulations.

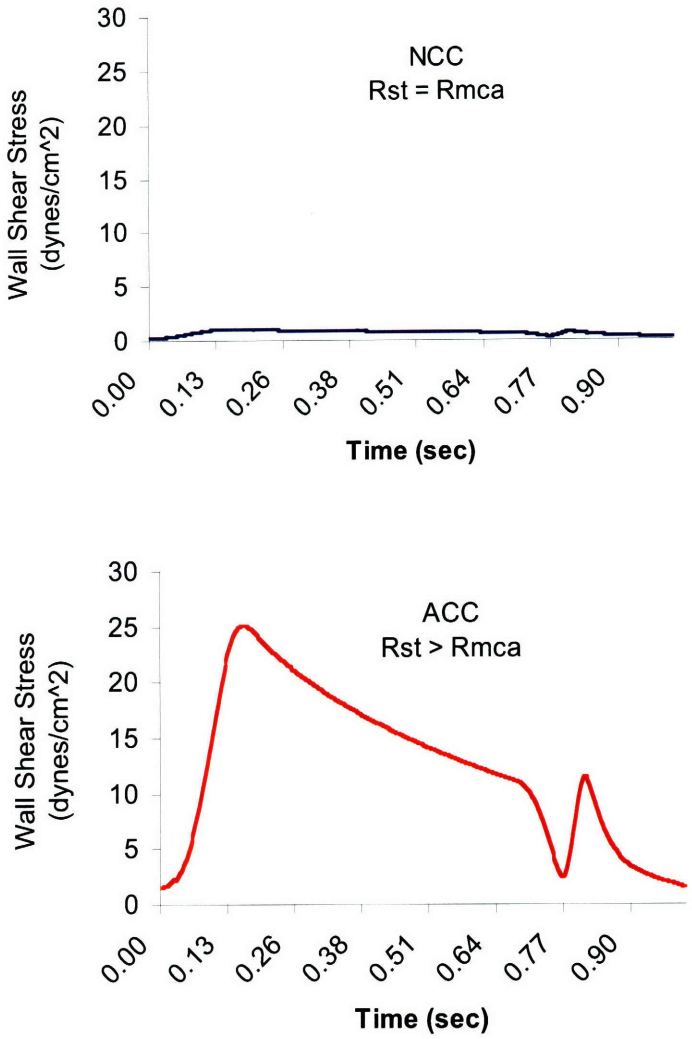

Figure 2.4 Both a normal coronary collateral waveform (NCC), where the resistance through the stenosis, R_{st}, equaled the resistance through the main coronary artery, R_{mca}, and an arteriogenic coronary collateral waveform (ACC), where the resistance through the stenosis, R_{st}, was equivalent to a 60% radius reduction of the main coronary artery, were generated with the lumped parameter coronary circulation model. The prototypic collateral waveforms are pulsatile over one cardiac cycle, with the NCC waveform having a mean shear stress value of 0.7 dyne/cm^2 and the ACC waveform having a mean shear stress value of 12.4 dyne/cm^2.

The two simulated coronary collateral waveforms displayed patterns consistent with the coronary circulation, in which shear stress (a value directly proportional to flow rate under Poiseuille flow assumptions) reaches maximum levels during diastole. This is in contrast with the peripheral or central circulation where the maximum blood flow occurs during systole as blood is ejected from the heart. The maximum shear stress corresponds to the portion of the cardiac cycle in which the external pressure (estimated from the pressure within the left ventricle) applied at the level of the capillaries is low. Conversely, the minimum shear stress magnitudes occur during systole when the external pressure acting on the capillaries is the greatest. This inverse relationship between external pressure acting on the coronary capillaries and collateral shear stress can best be explained by recognizing that the effective capillary resistance increases and decreases according to changes in the external pressure. Thus, as the myocardial pressure increases during systole, so does the external pressure acting on the capillaries and the effective capillary resistance and, even though aortic pressures driving flow are maximum during systole, the increase in capillary resistance significantly restricts blood flow through the coronary circulation during this portion of the cardiac cycle. Calculating the time-varying flow rates through the arteriolar and capillary vascular segments across the cardiac cycle further highlights the effect of myocardial contractile forces on coronary flow (Figure 2.5). The time-varying flow rate through the coronary arteriole segment has a pattern similar to the collateral flow rate or shear stress pattern, with the maximum flow occurring during diastole. In contrast, the capillary flow rate is maximum during systole as fluid is forced from the capillary vessels by the high external pressure and minimum during diastole as the external pressure diminishes. The maximum coronary arteriole flow during diastole therefore reflects rapid filling and storage of blood in the capillaries. In summary, although the lumped parameter model does

not provide details on the local hemodynamics of human coronary collaterals, it does have the capability to capture important features of the coronary circulation, including forces generated during myocardial contraction and alterations in blood flow that occur as a result of coronary artery disease.

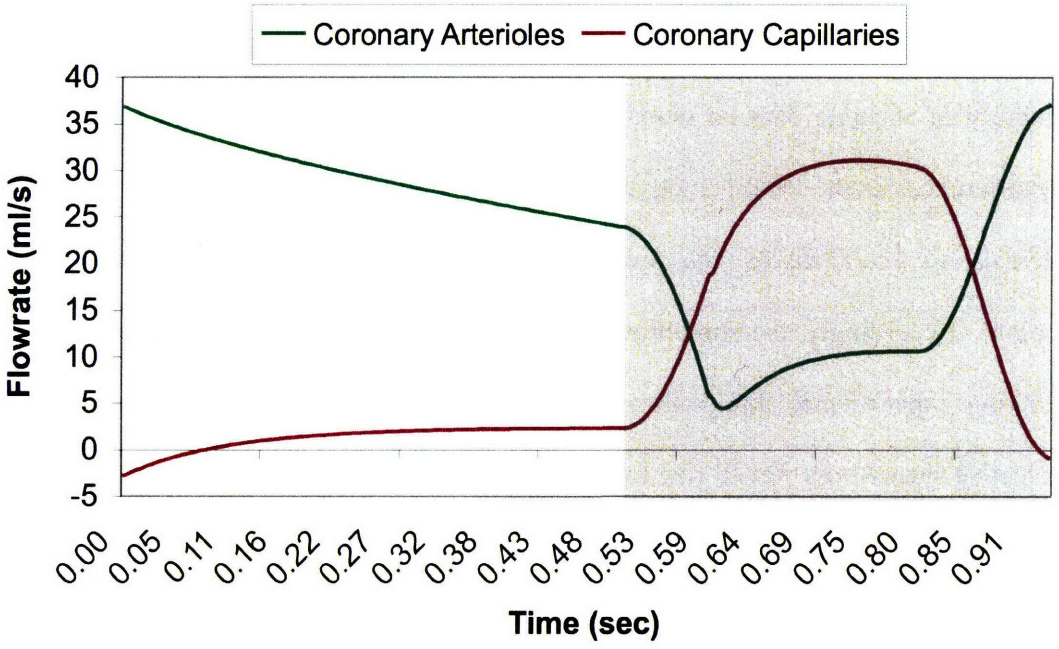

Figure 2.5 Flow rate data obtained from the lumped parameter model during the arteriogenic coronary collateral (ACC) simulation for the coronary arteriole coronary capillaries show flow patterns consistent with the coronary circulation where arteriole flow is greatest during diastole and capillary flow is greatest during systole (shaded portion) when the external pressure associated with myocardial contraction is maximal.

2.4 Discussion

Overall, the lumped parameter numerical simulations of coronary collateral hemodynamics represent two previously undefined shear stress waveforms relevant to collateral flow and coronary artery disease in humans. As a lumped parameter model, these waveforms provide a

bulk approximation of the biomechanical shear stress experienced by collateral vessels while neglecting the entrance, branch point, and inertial effects on collateral flow. Despite this, the bulk estimates of collateral waveforms are particularly suitable for studying effects collateral flow has on vascular cell phenotypes during arteriogenesis since vascular remodeling in this context occurs throughout the majority of the collateral vessel, rather than in distinct local locations (i.e. collateral entrance region). Furthermore, the simulation approach was dictated by the availability of accurate data on human collateral geometry and blood flow. As a counter example, differences in the local hemodynamics are thought to contribute to the focal nature of atherosclerosis, a vascular disease that predominantly has a non-random distribution at vascular branch points. Accordingly, the appropriate computational fluid dynamic approach for previous studies linking experimental data with numerical simulations characterizing atheroprone and atheroprotective shear stress waveforms was finite element analysis since MRI information from human subjects could be used to solve for these local shear stress waveforms with a resolution on the order of 100 μm (39). Similarly, based both on the desired shear stress resolution for each vessel and accessibility of critical model parameters, the lumped parameter model generated here constitutes an appropriate approach for numerically simulating the coronary collateral circulation.

Several approximations and assumptions were made in generating the lumped parameter model with regard to the coronary circulation hemodynamic parameters and collateral vessel geometry (i.e. collateral geometry and vessel resistances), as discussed in the Introduction and Methods sections. However, a number of fluid dynamic assumptions inherent to the lumped parameter model and shear stress calculation were also made in order to consider the flow one dimensional, laminar, and viscous. First, the complex secondary flows that result from vessel

bifurcation and curvature, as well as myocardial wall motion, were neglected. This was justified by determining both the Womersley number, a non-dimensional ratio between unsteady forces and viscous forces, and the Dean number, a non-dimensional measure of the centrifugal forces to the viscous force, to be small for reasonable values of the angular frequency (less than 10,000 rad/s) and the collateral radius to curvature ratio (< 1), as used to calculate the Womersley and Dean numbers, respectively (54). Also, using values from the lumped parameter model to estimate the Reynolds number, the non-dimensional measure of the inertial to viscous forces, yielded a value of < 1, lending further support of the fluid dynamic assumptions associated with viscous flow used here (54).

Although the coronary collateral simulation is novel in its current form, next generation iterations could be made to better account for the progressive hemodynamic changes that occur in these specialized vessels though out the arteriogenic processes. One possible modification would be to account for the early increases in collateral vessel diameter observed in femoral artery ligation models used to study arteriogenesis. The numerical simulation of coronary hemodynamics generated here assumed a fixed collateral radius for the normal coronary collateral (NCC) and partial stenosis/arteriogenic coronary collateral (ACC) waveforms. Although an instantaneous occlusion, which occur following hind limb femoral artery ligation, may not necessarily represent collateral development in the human, this type of occlusion has been shown to generate a rapid spike in collateral flow, which subsequently triggers acute, nitric oxide-mediated vasodilation (55). Thus, throughout the time course (~ days) of total occlusion-mediated collateralization, the collateral vessel shear stress presumably begins at a relatively low level prior to the occlusion, spikes at the moment of occlusion to a level that may induce mechanisms associated with vascular injury, and then returns to an intermediate level as the

collateral lumen expands and the vessel wall stabilizes. Considering the two distinct stages of arteriogenesis, with the first characterized by rapid vasodilation and inflammatory cell infiltration and the second characterized by vessel stabilization and maturation, it is possible that the first (inflammatory) stage correlates with the spike in collateral shear where as the second (maturation) stage correlates with the intermediate shear regime following the initial vasodilation (9).

In its current form, the coronary collateral simulation developed here does not attempt to simulate a complete main coronary artery occlusion, as would be required if the goal had been to model the hind limb femoral artery ligation models, since the shear stress magnitudes resulting from such a simulation are roughly two orders of magnitude greater compared to arterial levels and it is unclear if mature collaterals in the human heart most often develop following a total occlusion or as a result of progressive coronary artery disease with a partial occlusion. Rather, the present waveforms represent two distinct shear stress patterns characteristic of shear stress patterns experienced by the collateral endothelium with a constant vessel diameter in both the absence and presence of a partial main coronary artery occlusion. In order to conduct a realistic total occlusion simulation and relate it to experimental data, expansion of the collateral vessel diameter would need to be incorporated into the model, which would partially counteract the initial spike in collateral shear stress. Therefore, modifying the numerical simulation to reflect these transient changes in coronary collateral waveforms may later prove useful for elucidating the time-dependent mechanisms of arteriogenesis resulting from biomechanical stimulation. Moreover, the precise interpretation of how collateral waveform contributes to events of the different stages of arteriogenesis will ultimately require experimental results characterizing collateral flow control over vascular cell phenotypes, as is addressed in the following Chapters.

Chapter 3: Collateral Flow Regulates Vascular Cell Molecular Phenotypes

3.1 Introduction

As the single cell layer lining the lumen of blood vessels, the vascular endothelium provides an adaptive interface between flowing blood and the vessel wall that can sense local changes in the hemodynamic environment. The response of the endothelium to shear stress can occur rapidly over seconds or minutes through the activation of signaling mechanisms such as ion channels or the phosphorylation of intracellular kinases, while other endothelial cell responses to shear occur over much longer time scales such as the regulation of gene expression and cellular identity. Moreover, the diverse responses of the endothelium to shear stress are able to coordinate critical vascular functions, including inflammation, thrombosis, vasomotor tone, oxidative stress, and adaptive remodeling. Transcriptional profiling of endothelial cells stimulated in culture by well-defined shear stress waveforms has facilitated the identification and characterization of

numerous flow-mediated endothelial genes involved with regulating these critical vascular functions. The first endothelial microarrays used to determine shear-mediated endothelial phenotypes typically compared the gene expression profiles of endothelial cells grown under static conditions to endothelial cells exposed to steady arterial levels of shear stress. These early arrays contained far fewer measurable genes than the microarrays used today, but nevertheless they were able to detect a number of important flow-responsive genes (i.e. Cytochromes P450 A1 and B1, CyP1A1 and CyP1B1; monocyte chemotactic protein 1, MCP-1; and endothelin 1, ET-1/End1, actin, and cyclins) that have proven to be important for regulating vascular function (32,33,56). More recently, microarray analysis of endothelial cells subjected to various patterns of shear stress in culture have revealed important insights into the biomechanical regulation of endothelial cell proliferation and cytoskeletal composition, as well as inflammatory, thrombotic, and oxidative stress genes important for atherosclerosis (39,57,58). When used in combination with genetic manipulation (i.e. RNA interference), endothelial transcriptional profiling can also elucidate important mechanistic insights into the molecular regulation of the endothelial response to shear stress (40,57,59). Moreover, the power of transcriptional profiling, as used today, is in the identification of groups of genes that regulate common cellular functions and as an exploratory tool for providing direction in the study of a specific biological process.

One critical response of the endothelium to biomechanical force is the regulation of genes and activation of signals that may influence smooth muscle and perivascular cells within the vessel wall. Communication from the endothelium to the surrounding smooth muscle plays an important role in determining the phenotypic state of vascular smooth muscle cells, which functionally contributes to the endothelial control over vascular remodeling, vasomotor tone, and vascular development. Smooth muscle cells within the vessel wall reside along a phenotypic

continuum between a fully differentiated "contractile" phenotype in healthy vessels to a "synthetic" phenotype associated with vascular disease. Humoral signals, extracellular matrix composition, biomechanical forces, and heterotypic cell contact all contribute to determining the relative position of smooth muscle cells along this phenotypic continuum (60). Switching from a "contractile" to a "synthetic" SMC phenotype occurs in setting of vascular disease and is molecularly characterized by the downregulation of SMC-specific contractile proteins, including alpha-Smooth muscle actin, smooth muscle Myosin heavy chain, Calponin, and Desmin. The molecular changes in SMC associated with phenotypic switching to a "synthetic phenotype" correspond to functional changes as well, including increased migration, proliferation, and matrix production. It is also known that the transcriptional co-activators Myocardin and Serum-response factor (SRF) regulate expression of the majority of SMC contractile proteins by binding to their promoter and inducing transcription. More recently, smooth muscle Kruppel-like factor 4 (KLF4) has also been implicated as critical regulator of smooth muscle contractile protein expression by competing with Myocardin/SRF and acting as a repressor on the promoters of contractile genes (22).

The complex phenotypic plasticity displayed by smooth muscle cells both *in vivo* and *in vitro*, depends, at least in part, upon signals generated by the endothelium. In experimental co-culture systems, the endothelium has been shown to induce both smooth muscle cell migration and differentiation, as determined by the expression of Myocardin, alpha-Smooth muscle actin, and Calponin (19), suggesting that the endothelium can direct or contribute to maintaining a contractile smooth muscle cell phenotype. Furthermore, studies with endothelial cells grown under static conditions, Platelet-derived growth factor (PDGF), Transforming growth factor beta (TGF-β), Heparin-binding Epidermal growth factor (HB-EGF), and Interleukin-1 (IL-1) have all

been shown to influence smooth muscle cell gene expression, migration, and proliferation (19,61,62). More recently, shear stress acting on the endothelium has been shown to further promote increased expression of smooth muscle cell contractile genes (63), while repressing endothelial cell-induced smooth muscle migration (64,65). Taken together, it is clear that the endothelium has an important regulatory role in controlling smooth muscle phenotypes that can be altered by the presence of biomechanical forces, but a number of open questions remain regarding the flow-mediated endothelial mechanisms that lead to the observed effect of smooth muscle phenotypes, as well as the consequences of these endothelial-derived signals in the specific context of adaptive remodeling and other vascular processes that involve endothelial-smooth muscle cells interactions.

In an effort to better define how shear stress acting on the endothelium regulates arteriogenesis, the collateral waveforms numerically simulated in Chapter 2 were next experimentally applied to cultured endothelial cells for the purposes of (i) obtaining endothelial transcriptional profiles that may provide new insights into the molecular mechanisms that regulate endothelial-smooth muscle cell interactions relevant to adaptive remodeling and (ii) characterizing the effect of collateral flow-mediated endothelial paracrine signals on smooth muscle cells phenotypes. Accordingly, Chapter 3 discusses the molecular and functional changes evoked in vascular cells by collateral flow and the biological tools used to evaluate such changes.

3.2 Methods

3.2.1 Endothelial cell culture

Primary human umbilical vein endothelial cells (EC) were isolated, cultured, and subjected to shear stress waveforms as previously described (39). Briefly, EC, cultured in Medium-199 (BioWhittaker) supplemented with 50 mg/ml endothelial cell growth supplement (Collaborative Research), 100 mg/ml heparin (Sigma), 100 units/ml penicillin plus 100 m g/ml streptomycin (BioWhittaker), 2 mM L-Glutamine (GIBCO), and 20% FBS (BioWhittaker), were plated at an initial density of 70,000 cells per cm^2 on 0.1% gelatin (Difco)-coated polystyrene plastic disks (Plaskolite, Columbus, OH) and maintained at 37° C and in 5% CO_2 for 24 hours of static culture. After 24 hours, the static EC growth medium was exchanged for shear medium (Medium-199, 2% FBS, 2 mM L-Glutamine, 100 units/ml penicillin plus 100 m g/ml streptomycin, and 2.8 % dextran (Invitrogen)) with a viscosity of 2.2 cP. Exclusion of endothelial cell growth supplement and heparin, and the reduction of FBS to 2%, in the shear medium were required to minimize the effect media supplements have on smooth muscle cell phenotype and function during conditioned media experiments. EC shear stress application, using the NCC and ACC shear stress patterns in the *dynamic flow system,* was initiated within one hour of the medium exchange (Figure 3.1). While applying shear stress to EC, the shear medium was maintained at 37° C and was continually exchanged at a volumetric flow rate of 30 µl/minute and the entire *dynamic flow system* excluding the motor used to drive the cone motion is contained in a 5% CO_2 environment.

3.2.2 Smooth muscle cell culture and delivery of conditioned medium

Human aortic vascular smooth muscle cells (SMC) (ATCC, CRL-1999) were grown and propagated in complete growth medium according to the supplier's instructions. For experiments in which conditioned medium containing flow-mediated endothelial-derived factors was continuously delivered to SMC, 100,000 SMC were plated on 0.1% gelatin (Difco)-coated glass coverslips (25 x 75mm #1, Belco) 24 hrs prior to exposure to conditioned media and maintained in serum-free medium (complete growth medium with the 10% FBS removed) at 37 ^{o}C and 5% CO_2 (Figure 3.1). On the day of experimentation, ACC and NCC shear stress waveforms imposed on EC were initiated in the *dynamic flow system* 1 hr prior to connecting to the downstream SMC culture chamber via 1% bovine serum albumin (BSA, Sigma)-coated Tygon tubing. No endothelial control experiments were conducted with SMC grown and maintained in the same culture chamber, but in the absence of upstream EC.

Specific design considerations for the two dimensional SMC acceptor chamber were made in order to control the biomechanical environment such that the wall shear stress experienced by smooth muscle cells does not exceed fluid shear stress mechanical activation thresholds for adherent cells and that mass transport of small molecules within the chamber is dominated by convection. With a parallel plate outflow chamber geometry of 60 cm x 1.75 cm x 0.025 cm (L x W x H), a fluid viscosity (μ) of 2.2 cP, and an average flow rate (Q) of 30 μl/minute, the wall shear stress τ can be calculated assuming viscous, one-dimensional, fully developed (entrance length ~ 0.01 cm) Newtonian flow in the long axis direction using the equation $\tau = (6\mu Q)/(h^2 w)$. Based on this calculation, the average wall shear stress experienced

by plated smooth muscle cells is less than 0.1 dyne/cm^2. Next, assuming a reasonable value for protein diffusion in a liquid (D ~ 0.1 mm^2/hr), comparison of the relative contribution of convection to diffusion using the dimensionless Peclet number (Pe = UL/D ~ 10^5, where U is the average velocity) reveals that mass transport is dominated by convection. Thus, it is assumed that negligible gradients of endothelial-derived products develop in the axial direction of the *acceptor chamber* and that once steady state is reached a stable concentration profile for small molecules will exist in the vertical direction.

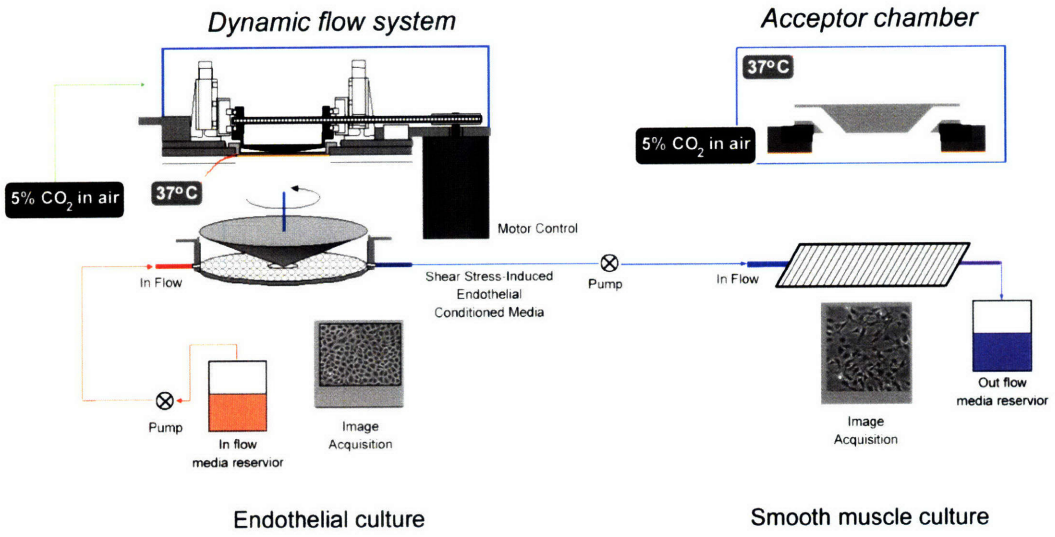

Figure 3.1 Schematic of the *mechano-activated paracrine bioassay system* that combines a *dynamic flow system* to apply precise shear stress patterns to cultured human endothelial cells and deliver the flow-mediated conditioned medium to a two dimensional smooth muscle cell *acceptor chamber*.

3.2.3 Flow cytometry analysis of cell cycle

The DNA profiles of apoptotic and viable SMC were assessed by measuring the fluorescent intensity of propidium iodine (PI) for each cell. Cells were collected after trypsinization, centrifuged, and washed with PBS containing 2% FBS. Cells were then fixed in ice-cold ethanol

(70%) at -20°C for a minimum of 4 hr. After fixation, cells were pelleted, washed with PBS containing 2% FBS, and then resuspended in a staining solution that contained PBS with 2% FBS, 1 mg/ml of ribonuclease (RNAse) A (84.4 U/mg), and 50 μg/ml of PI. The resuspended cells were then kept at 37° C for 30 minutes. Following the incubation, cells were washed with PBS containing 2% FBS. The DNA content was immediately measured by flow cytometry from 10,000 events per experimental and the results were analyzed using CellQuest software, with number of cells in the G_1, S, or G_2/M cell cycle phases or undergoing apoptosis expressed as a percentage of total cells.

3.2.4 Transcriptional profiling

For microarray experiments, cells were lysed using Trizol reagent and RNA was isolated by ethanol precipitation, DNase treated, purified on a column (Quiagen). RNA for the SMC microarray was subjected to one round of linear amplification, starting with 0.5 μg, using the NanoAmp RT-IVT (reverse transcription-in vitro translation) kit according to the manufacturer's instructions (Applied Biosystems). Labeling, hybridization and scanning of microarrays for ACC versus NCC flow-stimulated EC transcriptional profiling or SMC exposed to ACC versus NCC flow-mediated EC conditioned medium was performed according to the manufacturer's protocols for the ABI1700 microarray system using total genome microarrays containing 30,096 spots representing 28,790 distinct genes (Applied Biosystems) and as previously described (40). The n. Differential regulation of NCC and ACC flow-mediated EC genes was then analyzed in custom-designed Matlab (Mathworks) software for significance using 3 replicate experiments and Z-pool statistical methodology, defining statistically significant gene regulation for $P < 0.001$ (66). Differentially regulated genes were then sorted by biological function using the

publicly-available Panther database (www.panther.org; Applied Biosystems) and cross-referenced with the Gene Ontology classification (http://www.geneontology.org/). The microarray data were submitted as a dataset series to the Gene Expression Omnibus (GEO) (Accession number GSE11583). For the SMC microarray, a single exploratory array was performed. For this sample, the microarray raw signal values were filtered for signal to noise quality and normalized using Lowess regression and differentially regulated genes were selected by fold-change and raw intensity. Selected genes were then validated using TaqMan real-time PCR from separate, not amplified samples.

3.2.5 RNA preparation and RT-PCR analysis

Total RNA from EC and SMC used for TaqMan real-time PCR was isolated using Lysis Buffer (Applied Biosystems) and purified using the Prism Nucleic Acid Prep-Station (Applied Biosystems) according to the manufacturer's instructions. RNA quantity was measured by spectrophotometic analysis at 260 nm and quality was verified by Agilent's 2100 Bioanalyzer with RNA 6000 Nano LabChip Kit. Purified, DNase-treated RNA (0.375 μg) was reverse-transcribed using a MultiScribe-based 25 μl reaction (Applied Biosystems). The cDNA was diluted in 50 μl DNAse-free water and subjected to a 20 μl real-time TaqMan quantitative PCR (Applied Biosystems 7900). Expression of EC Kruppel-like factor 2 (KLF2, ABI TaqMan probe Hs00360439_g1), Tyrosine-protein kinase receptor Tie2 (Tie2, ABI TaqMan probe Hs00176096_m1), Nephroblastoma overexpressed protein (NOV, ABI TaqMan probe Hs00159631_m1), Angiopoietin 2 (Ang2, ABI TaqMan probe Hs00169867), and Connective tissue growth factor (CTGF, forward primer 5'- CCAAGGACCAAACCGTGGTT-3', reverse primer 5'- ATAGTTGGGTCTGGGCCAAAC-3', TaqMan probe 5'-

CCCTCGCGGCTTACCGACTGG-3'), and expression of SMC Myocardin (MYOCD ABI TaqMan probe Hs00538076_m1) and Matrix metalloproteinase 3 (MMP3, ABI TaqMan probe Hs00968308_m1), were reported relative to GAPDH (ABI TaqMan probe Hs99999905_m1).

3.2.6 Statistical analysis

Statistical significance was determined by one-way ANOVA for experiments with more than two subgroups, while *post hoc* and pairwise comparisons were performed by 2-tailed Student's *t* test for all others (Primer of Biostatistics). *P* values less than 0.05 were considered significant. Statistical significance for the microarray data is described in the *Transcriptional profiling* subsection.

3.3 Results

3.3.1 Collateral shear stress regulates endothelial gene expression patterns

The two simulated coronary collateral waveforms developed in Chapter 2 were applied to cultured human umbilical vein endothelial cells (EC) for 24 hr and differences in the resulting EC molecular phenotype were determined by genome-wide transcriptional profiling. In total, 681 genes were found to have statistically significant regulation, as determined by Z-pool P values less than 0.001 (Figure 3.1A) (66). Further analysis revealed the differential regulation of multiple endothelial genes that have previously been shown to influence both acute and chronic vascular adaptations in the developing embryo and the adult (Table 3.1). This collateral flow-mediated endothelial gene expression pattern included the differential regulation of vasoactive,

angiogenic, inflammatory, extracellular matrix, developmental, secreted, and transcription factor genes. Specifically, ACC flow upregulated expression of vasodilatory genes (endothelial Nitric oxide synthase, eNOS; and Vasoactive intestinal peptide, VIP), endothelial receptors and ligands required for arterial development (endothelial Tyrosine kinase receptor, Tie2 and Jagged 1, Jag1), extracellular matrix regulators (Nephroblastoma overexpressed, NOV; Tissue inhibitor metalloproteinase 3, TIMP3), and transcription factors (KLF2, KLF10, KLF13; and Forkhead box f1, FOXF1). Conversely, ACC flow downregulated endothelial genes involved with angiogenesis/wound healing (Angiopoietin 2, Angpt2/Ang2; Fibulin 5, FBLN5; Interleukin-8, IL8; Connective tissue growth factor, CTGF; Cysteine rich 61, CyR61; Semaphorin 3A, Sema3A; Transforming growth factor beta2, TGFB2; and Neuropilin 1, NRP1), inflammation (Monocyte chemotactic protein 1, MCP-1; Interleukin-8, IL8; Bone morphogenic protein 4, BMP4; and Bone morphogenic protein 2, BMP2), transcription (Forkhead box o1a; FOXO1A) and vasoconstriction (Endothelin 1, END1/ET-1).

The collateral flow-mediated transcriptional profiling data, cross-referenced with previously published endothelial microarray datasets by Parmar et al, also revealed that a significant proportion of these collateral flow-mediated genes, both up- and downregulated, are transcriptional targets of the endothelial transcription factor Kruppel-like Factor 2 (KLF2) (genes italicized in Table 1) (40). Additional transcription factors were also found to be differentially regulated by the collateral waveforms (See Appendix) and none of the ones upregulated by the ACC waveform had as substantial published evidence as KLF2 for controlling the formation and maintenance of the vessel wall (17,47). Thus, KLF2 emerged from the analysis as a collateral-flow regulated transcription factor that may act as a central regulator of endothelial-dependent events critical for adaptive arterial remodeling. The upregulation of KLF2 by the ACC

waveform was confirmed by TaqMan real-time PCR along with several genes that we have previously shown to be dependent on KLF2 expression, including the upregulation of endothelial Tyrosine kinase receptor (Tie2) and Nephroblastoma overexpressed (NOV) and the downregulation of the vascular de-stabilizing/pro-angiogenic genes Angiopoietin 2 (Angpt2) and Connective tissue growth factor (CTGF) (Figure 3.2B). Collectively, these transcriptional profile expression patterns demonstrate that collateral flow promotes a distinct endothelial molecular phenotype associated with mature, arterial vessels and provide a comprehensive collection of collateral flow-mediated endothelial genes that may exert a regulatory role in adaptive remodeling.

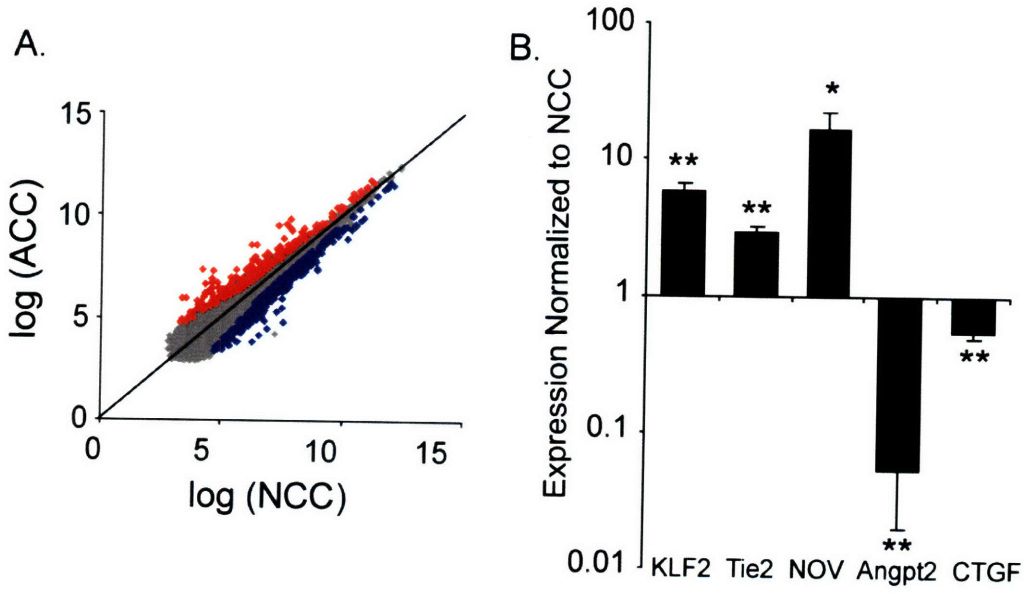

Figure 3.2 Collateral flow regulates vascular cell molecular phenotypes. A) Application of the simulated coronary collateral waveforms to cultured human endothelial cells resulted in genome-wide differences in endothelial transcriptional profiles. Significant differences across 3 independent samples were determined statistically for $P < 0.001$, using a Z-statistic method of pooled variances. Normalizing ACC gene expression to NCC yielded 267 significantly upregulated genes (red) and 414 significantly downregulated genes (blue). B) Real-time TaqMan PCR validation of select differentially regulated genes identified by the transcriptional profiles as having a potential role in adaptive remodeling. KLF2 = kruppel-like factor 2; Tie2 = tyrosine kinase receptor (endothelial); NOV = nephroblastoma overexpressed; Angpt2 = angiopoietin 2; CTGF = connective tissue growth factor. Data represent the mean of 4 independent experiments. All error bars reported as standard error with * $P < 0.05$ and ** $P < 0.01$.

	RefSeq	Gene Name; Symbol	Fold Change	Remodeling Function
Up	NM_002514.2	*nephroblastoma overexpressed gene;NOV* *	26.5472	matricellular protein; ECM protein
	NM_194435.1	vasoactive intestinal peptide;VIP	4.7390	vasodilation; secreted peptide
	NM_016270.1	*kruppel-like factor 2 (lung);KLF2*	4.5575	vasoprotection; transcription factor
	NM_000362.3	tissue inhibitor of metalloproteinase 3; TIMP3	3.7926	anti-angiogenesis; ECM remodeling
	NM_000603.3	*NOS3 - nitric oxide synthase 3 (endothelial cell)* *	2.9320	vasodilation
	NM_000459.1	*tyrosine kinase, endothelial; TEK/Tie2* *	2.6057	vascular development; receptor
	NM_00214.1	jagged 1 (Alagille syndrome);Jag1	2.2904	vascular development; notch ligand
	NM_002006.3	fibroblast growth factor 2 (basic);FGF2	2.2724	angiogenesis/arteriogenesis; secreted
Down	NM_003873.2	neuropilin 1;NRP1	-2.1897	angiogenesis; secreted
	NM_003239.1	transforming growth factor, beta 2;TGFB2	-2.1517	wound healing; secreted
	NM_001554.3	*cysteine-rich, angiogenic inducer, 61;CYR61* *	-2.2162	angiognesis; secreted
	NM_130851.1	*bone morphogenetic protein 4;BMP4* *	-2.5047	inflammation; secreted
	NM_006080.1	semaphorin 3A;SEMA3A	-2.5114	angiogenesis; secreted
	NM_001200.1	bone morphogenetic protein 2;BMP2	-2.5437	inflammation; secreted
	NM_001901.1	*connective tissue growth factor;CTGF* *	-2.6762	wound healing; secreted
	NM_001955.2	*endothelin 1;EDN1* *	-3.0242	vasoconstriction; secreted
	NM_000584.2	*interleukin 8; IL8* *	-3.5467	inflammation; cytokine
	NM_006329.2	fibulin 5;FBLN5	-3.6664	angiogenesis; ECM protein
	NM_002983.2	*chemokine (C-C motif) ligand 2; CCL2 (MCP-1)* *	-4.6387	inflammation; cytokine
	NM_001147.1	*angiopoietin 2;ANGPT2* *	-9.9658	angiogenesis; secreted

Table 3.1 *Differential expression of collateral flow-mediated endothelial genes identified by transcriptional profiling and associated with adaptive remodeling.* * Genes listed in italics are previously defined transcriptional targets of KLF2 (40). ECM = extracellular matrix.

3.3.2 Collateral flow acting on the endothelium regulates smooth muscle cell gene expression, but not proliferation

In order to determine whether the simulated collateral flow waveforms acting on EC have the downstream capacity to differentially regulate smooth muscle gene expression, a vascular cell co-culture system was developed that supports the culture of human aortic smooth muscle cells (SMC) while receiving flow-mediated EC conditioned medium (Figure 3.1). The SMC aspect of the culture system was continuously perfused throughout the duration of a collateral flow experiment without allowing direct contact between EC and SMC, thereby excluding effects mediated by cell-cell interactions. With the system, the effect of flow-mediated endothelial secreted factors on SMC gene expression and proliferation were evaluated.

Initially, transcriptional profiling of SMC exposed to NCC versus ACC flow-mediated EC conditioned medium for 24 hr was performed and analyzed for genome-wide differences in SMC gene expression. To obtain the transcriptional profiles, a single exploratory microarray was performed on each sample using SMC expression of Myocardin (MYOCD), a transcriptional co-activator essential for the expression of multiple SMC contractile proteins (Figure 3.3A) (60), as a sentinel gene for ensuring SMC responsiveness to the different conditioned media. Preliminary studies had revealed that ACC flow-mediated EC conditioned medium approximately leads to a two-fold induction of Myocardin. Also, RNA used for the transcriptional profiling was first subjected to one round of linear amplification. With the single microarray dataset, the Z-pool analysis used to identify statistically regulated genes from the endothelial transcriptional profile experiments could not be performed. Rather, three criteria were used for selecting differentially regulated SMC genes for validation, which included:

1. Fold change – Genes with less than 3-fold difference between ACC and NCC samples were excluded.
2. Raw intensity – For the Applied Biosystems 1700 microarray, spot intensities less than 1000 arbitrary fluorescent intensity units were flagged as unreliable and genes from the ACC and NCC samples that both had raw intensity values of less than 1000 were excluded.
3. Biological relevance – Genes without a known biological role related to vasomotor tone, cyoskeletal protein, extracellular matrix production or other biological functions associated with vascular remodeling were excluded.

The genes selected for further validation included GTP-cyclohyrolase 1 (GCH-1), Laminin C2 (LamC2), and Matrix metalloproteinase 3 (MMP3) (Table 3.2). Myocardin was also found to be upregulated by ACC collateral flow-mediated endothelial conditioned medium on the exploratory array, but only by 1.4 fold. Similarly, alpha-Smooth muscle actin (Acta2/αSMA), a transcriptional target of myocardin, was upregulated by a fold induction that did not meet the gene selection criterion, but the biological relevance of Acta2 with regard to SMC phenotypic precluded the gene from exclusion. Validation of the selected SMC genes, as well as myocardin and alpha-Smooth muscle actin, was performed using TaqMan real-time PCR with samples from four separate experiments, including no endothelium control SMC samples. Results from the PCR validation confirmed the observed changes in SMC gene expression for Myocardin and Matrix metalloproteinase 3, where as the two other genes identified (GCH1 and LamC2) displayed no change in expression (Table 3.2 and Figure 3.3). The difference in alpha-Smooth muscle actin expression, although increased in the ACC sample, was not found to be statistically significant (data not shown).

Gene ID	Gene Name	Microarray	RT-PCR
hCG22618.3	GCH1 - GTP cyclohydrolase 1	515.66	0.34
hCG40730.3	laminin, gamma 2 (LAMC2)	4.17	0.85
hCG22984.4	ACTA2 - actin, alpha 2, smooth muscle, aorta	1.81	2.2
hCG1811056.2	MYOCD - myocardin	1.44	2.29
hCG41473.3	MMP3 - matrix metalloproteinase 3 (stromelysin 1)	0.16	0.23

Table 3.2 *Validation of smooth muscle cell genes selected from exploratory microarray as differentially regulated by collateral flow-mediated endothelial conditioned medium and potentially important for arteriogenesis.* Myocardin (MYOCD), alpha-Smooth muscle actin (ACTA2/αSMC), and Matrix metalloproteinase 3 (MMP3) were verified using real-time TaqMan PCR, where as GTP cyclohydrolase I (GCH1) and Laminin (LAMC2) did not.

Myocardin expression levels provide a relative assessment of the SMC molecular phenotype resulting from flow-mediated EC paracrine factors, with increased expression of the genes corresponding to a more contractile SMC phenotype. This was observed for SMC exposed to ACC flow-mediated EC conditioned medium compared to NCC and no endothelial control media. The expression of MMP3, a matrix degrading enzyme whose expression is associated pathologic changes to the vessel wall and monocyte activity (67,68), is less well characterized for its role in determining SMC phenotypes, but downregulation of MMP3 in SMC in the ACC sample suggests a potential mechanism through which collateral flow regulates vascular wall stabilization.

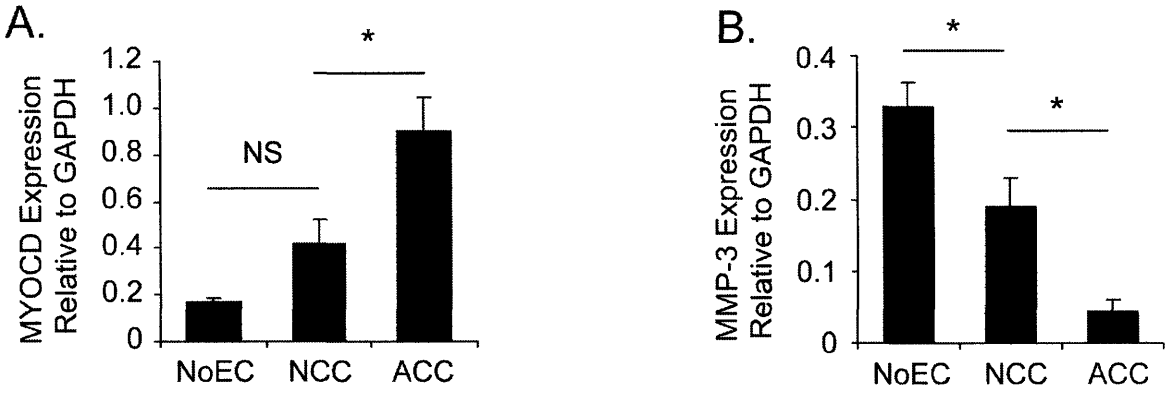

Figure 3.3 Conditioned medium from the simulated adaptive remodeling (ACC) compared to the normal (NCC) collateral waveform and a no endothelium control increased SMC gene expression of A) Myocardin (MYOCD) and decreased the expression of B) Matrix metalloproteinase 3 (MMP3), as determined by real-time TaqMan PCR. Data represent the mean of 4 independent experiments. All error bars reported as standard error with * $P < 0.05$ and ** $P < 0.01$.

Smooth muscle cell proliferation is an important SMC phenotype that has implications on the function and structure of the vessel wall. In order to evaluate the effect of collateral flow-mediated conditions medium on these functional SMC phenotypes, analysis of cell cycle progression as a relative indicator of proliferation was performed on propidium iodine-labeled cells using flow cytometry. Comparison of SMC exposed to ACC and NCC flow-mediated conditioned medium, as well as no endothelial control SMC, revealed that collateral flow acting on the endothelium does not affect SMC proliferation, at least for the co-culture system used for these experiments (Figure 3.4). As an additional positive control, SMC cultured in high serum content medium (20% FBS) displayed a significant increase in cell cycle progression. Multiple experimental conditions were varied in these experiments, including initial SMC seeding density and time of exposure to conditioned medium, with each variation resulting in the same conclusion. These results may indicate that collateral flow alone, in the absence of inflammatory cells and mediators, does not affect SMC proliferation or they may indicate the co-culture system in its current form does not have the sensitivity for SMC to sense differences in flow-mediated EC conditioned medium that can then induce changes in proliferation.

3.3.3 Summary

By coupling the simulated collateral waveforms with dynamic EC-SMC co-culture, the results from experiments summarized in this chapter demonstrate that collateral flow acting on the endothelium regulates global endothelial gene expression patterns consistent a mature, quiescent phenotype and that collateral flow-mediated endothelial conditioned medium has the capacity to modulate the expression of SMC contractile and extracellular matrix genes, but not proliferation. Taken together, these data suggest that flow acting on the endothelium is an important

determinant of vascular cell phenotype and the production of flow-mediated endothelial paracrine signals during adaptive remodeling evokes SMC gene expression consistent with arterial wall maturation and stabilization.

A.

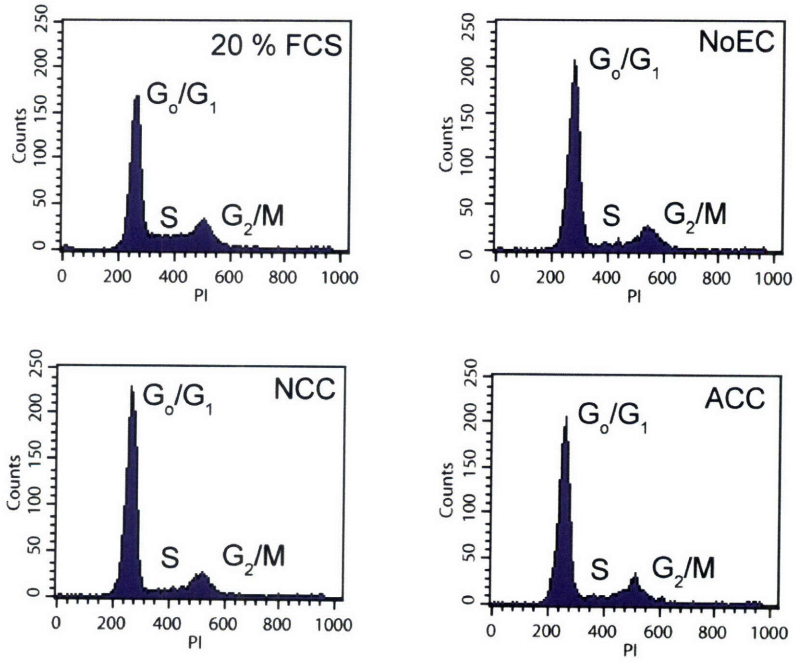

B.

	G_0/G_1	S	G_2/M
20% FCS	66.5%	9.5%	21.1%
NoEC	78.3%	2.5%	17.3%
NCC	79.8%	2.9%	15.4%
ACC	76.3%	3.8%	17.2%

Figure 3.4 Smooth muscle cell (SMC) proliferation in response to collateral flow EC conditioned medium was investigated by DNA labeling with propidium iodine and analyzing for cell cycle using flow cytometry. A) SMC cell cycle data was obtained for a serum stimulated positive control (20% FSC), a no endothelial control (NoEC), NCC flow-mediated EC conditioned medium, and ACC flow-mediated EC conditioned medium with 10,000 counts were used for each sample. B) Quantification of the percentage of cells in each phase of the cell cycle revealed that flow-mediated EC conditioned medium did not result in a significant change in SMC proliferation rates.

3.4 Discussion

Arterial remodeling is a dynamic function of the vasculature required to maintain systemic perfusion under both normal and pathological conditions. In some cases, such as coronary collateralization or adaptive arteriogenesis, local hemodynamics control specific cellular processes that lead to arterial remodeling. In order to address the question of how changes in flow acting on the collateral endothelium contributes to adaptive arteriogenesis, an experimental culture system was employed that applies numerically simulated coronary collateral waveforms to cultured endothelial cells while simultaneously delivering the resulting flow-mediated endothelial conditioned medium to smooth muscle cells. Using this experimental system, collateral flow was shown to evoke changes in endothelial gene expression relevant to adaptive remodeling and, through collateral flow-mediated endothelial paracrine signals, also modulate smooth muscle expression of genes associated with a mature smooth muscle phenotype.

Several of the endothelial genes characterized by genome-wide transcriptional profiling to be differentially regulated by the coronary collateral waveforms have previously been reported to regulate critical processes involved with adaptive remodeling. Specifically, the adaptive remodeling coronary collateral (ACC) waveform increased expression of genes important for vessel tone (eNOS and VIP), vascular development/remodeling (Tie2, FGF2, Dll1, and Jag1) and maintenance of the arterial extracellular matrix (NOV and TIMP3). Vasodilation of collateral vessels is critical to the initial stage of collateral adaptation and highly dependent on eNOS (55) in response to rapid increases in flow. *In vivo* evidence also supports a critical role for the Angiopoietin-Tie2 and Notch-Jag1/Dll1 receptor-ligand systems in both arterial development

and adaptive coronary remodeling (69-71). Furthermore, NOV has documented expression in stable large diameter arteries (72) and FGF2, a gene typically associated with angiogenesis, has recently been reported to promote collateralization and act synergistically with PDGF to stabilize newly formed vessels (73). The ACC waveform also downregulated multiple endothelial genes involved with angiogenesis/wound healing (Angpt2, FBLN5, IL8, CTGF, Cyr61, Sema3A, TGFB2, NRP1), inflammation (IL8, MCP-1), and vasoconstriction (END-1) compared to the NCC waveform. Angiogenic and inflammatory genes are often associated with vascular remodeling, particularly in ischemic tissue or during pathological remodeling, but these processes may have detrimental effects to adaptive remodeling since their stimuli and end-product vessel structure and function differ significantly. Consistent with the concept that endothelial genes downregulated by ACC flow would have detrimental effects on adaptive remodeling is the observation by Reiss et al that constitutive overexpression of Angiopoietin-2, a pro-angiogenic endothelial gene, in animals subjected to hind limb femoral artery ligation dramatically impairs collateral vessel remodeling (74). Therefore, combining the collateral flow-mediated endothelial transcriptional profile data documented here with *in vivo* evidence on the role of specific endothelial genes in vascular remodeling and development suggests that collateral flow has the ability to evoke distinct endothelial gene expression patterns whose functional contribution towards adaptive arteriogenesis may be through the stabilization and maintenance of large diameter arteries.

Comparison of the endothelial transcriptional profiles evoked by the arteriogenic (ACC) waveform to endothelial transcriptional profiles reported in previously published data (40) using waveforms with a similar magnitude of shear stress, specifically an arterial waveform derived from the region of the carotid bifurcation protected against atherosclerosis (39), provided further

evidence regarding the unique control that the ACC flow pattern has over endothelial gene expression. The transcriptional profile datasets for this comparison did not represent biological pairs and the media condition varied, but nevertheless paired analysis of the two arterial-level waveforms revealed the differential regulation of approximately 2000 genes, with a surprisingly large number of genes involved with Notch signaling downregulated by the ACC waveform compared to the waveform generated from the carotid artery (i.e. Hey1 and Hey2, Jagged 1, Dll1, Dll4, and Ephrin-B2). This may simply reflect the different media conditions between experiments since the ACC flow-stimulated cells were maintained in a reduced serum medium that did not contain endothelial cell growth stimulant (ECGS) or heparin, but it could also suggest that the biomechanical regulation of Notch signaling depends on the waveform specific to distinct regions within the arterial vasculature. None of the genes indentified on the endothelial transcriptional profile as differentially regulated by collateral flow and validated by PCR (KLF2 and KLF2 transcriptional targets), however, showed significant differences when comparing the ACC waveform to the carotid artery waveform. Furthermore, application of the mean value of ACC waveform to endothelial cells resulted in a similar upregulation of KLF2 as the pulsatile waveform (data not shown), suggesting that components of the collateral flow response by the endothelium applies more generally to vessels with similar magnitudes of wall shear stress.

Collateral flow applied to the endothelium also has the capacity to regulate paracrine signals that evoke changes in smooth muscle cell gene expression, as shown by delivering conditioned medium from the collateral flow experiments to cultured SMC. In particular, the ACC waveform resulted in increased SMC expression of Myocardin (MYOCD) and decreased expression of Matrix metalloproteinase 3 (MMP3). Myocardin is an important SMC nuclear co-

factor for maintaining a contractile SMC phenotype characteristic of stable large diameter arteries (60), while MMP3 is associated with breakdown of the vascular wall extracellular matrix during chronic vascular pathologies (68). Furthermore, gene expression data by Lee et al from femoral artery ligation experiments showed that MMP3 is downregulated in the ischemic hind limb during late-stage remodeling, which is consistent with the collateral flow regulation of SMC MMP3 and temporally correlated with the second stage of arteriogenesis (75).

Collectively, the gene expression patterns evoked by collateral flow in endothelial and smooth muscle cells suggest that collateral flow in the context of arteriogenesis promotes blood vessel stabilization and maturation by inducing genes associated with mature, large diameter arteries (i.e. NOV in EC and MYOCD in SMC) while suppressing genes involved with vascular destabilization processes (i.e. Angpt2 and CTGF in EC and MMP3 in SMC). Furthermore, data from the collateral flow-mediated EC and SMC gene expression experiments suggest that the arteriogenic collateral waveform simulated in Chapter 2 may best correlate with collateral flow during the stage of arteriogenesis characterized by vessel stabilization, vascular wall maturation and resolution of the initial inflammatory response.

Therapeutic control of vessel wall stabilization and maturation could have important clinical applications, including the promotion of coronary collateralization and tumor vasculature normalization. However, the data generated here does not mechanistically define any molecular targets to could be used achieve these effects. Current attempts at therapeutic arteriogenesis have primarily focused on stimulating the initial inflammatory responses and these efforts could potentially be improved if used in combination with molecular targets that regulate vessel stabilization and maturation. The endothelial transcription factor Kruppel-like factor 2 (KLF2) constitutes an attractive target of investigation for this aspect of therapeutic arteriogenesis based

on its documented role in regulating critical flow-mediated endothelial genes and in controlling vascular smooth muscle function *in vivo*, but experimental data does not exist specifically characterizing the effect of KLF2 expression in the endothelium on interactions with smooth muscle cells important for the vessel wall architecture. Accordingly, efforts described in Chapter 4 attempt to provide mechanistic insight into the endothelial response during arteriogenesis by defining smooth muscle functions controlled by endothelial expression of KLF2.

Chapter 4: Endothelial KLF2 Controls Smooth Muscle Migration

4.1 Introduction

Changes in hemodynamic shear stress contribute to coronary collateralization, yet molecular mechanisms controlling the endothelial response and coordinating cellular events that regulate adaptive arteriogenesis remain largely uncharacterized. The endothelial transcription factor Kruppel-like factor 2 (KLF2) emerged from the collateral flow-mediated EC transcriptional profile analysis in Chapter 3 as a potential key player in regulating an adaptive remodeling endothelial response based on evidence of its flow dependence and necessity to the function of the developing vessel wall. Furthermore, previous transcriptional profile data from others has documented that KLF2 regulates a significant proportion of flow-mediated endothelial genes, several of which were also differentially regulated by the collateral waveforms, including Nephroblastoma overexpressed (NOV), Angiopoietin 2 (Angpt2), Connective tissue growth Factor (CTGF), and endothelial Nitric oxide synthase (eNOS). A number of other endothelial transcription factors were also regulated by the ACC waveform (Supplemental Data), but KLF2 had the strongest *in vivo* evidence supporting a role in adaptive remodeling where mice lacking KLF2 display lethal phenotypes of impaired vascular maturation and function. In particular,

both complete and endothelial-specific knockout of KLF2 in mice results in embryonic lethality due to hemorrhage (17) and an inability to regulate vessel tone and hemodynamics (46), respectively, most likely through impaired smooth muscle function (47). None of these mouse models, however, lack the ability to form nascent vessels, implying that the principal vascular defect associated with KLF2 loss involves ineffective endothelial regulation of smooth muscle functions associated with vessel wall reactivity and stability. Thus, KLF2 may represents a potentially critical regulatory node in arterial remodeling and defining how endothelial KLF2 expression affects smooth muscle function could provide novel mechanistic insight into the biomechanical control of arteriogenesis.

Smooth muscle cells display extraordinary phenotypic plasticity, switching from a mature "contractile" phenotype to a de-differentiated "synthetic" phenotype in response to a number of local environmental cues. The relative state of a smooth muscle cell along the phenotypic continuum is characterized by gene expression, as well as patterns of migration and proliferation, as discussed in Chapter 3. Phenotypic switching of smooth muscle cells is relevant to a number of vascular pathologies and functionally manifests as changes in the vascular wall architecture due to increased smooth muscle cell migration and proliferation and decreased expression of contractile markers (60). The most well characterized examples of smooth muscle phenotypic switching in vascular disease occur during restenosis and atherosclerosis in which smooth muscle cells undergo aberrant proliferation and migration, leading to intimal hyperplasia and neointimal formation (76). As observed in Chapter 3, collateral flow acting on the endothelium promotes a "contractile" smooth muscle gene expression pattern, as opposed to the smooth muscle "synthetic" phenotype associated with restenosis and atherosclerosis, suggesting that the phenotypic changes undergone by smooth muscle cells during arteriogenesis are distinct from

those associated with pathological vascular remodeling. Thus, in order to gain mechanistic insight into the molecular mechanisms responsible for the generation of endothelial signals to smooth muscle cells during arteriogenesis, Chapter 4 focuses on defining the role of endothelial KLF2 expression in the regulation of a mature, contractile smooth muscle phenotype, as characterized by smooth muscle gene expression, proliferation, and migration.

4.2 Methods

4.2.1 Cell culture

Endothelial and smooth muscle cells were isolated, propagated, and maintained as described in the Methods section of Chapter 3. For siRNA experiments silencing KLF2 in EC and delivering collateral flow-mediated EC conditioned medium to SMC, the EC dynamic flow system and SMC acceptor chamber were used as described previously and in the Methods section of Chapter 3. For KLF2 overexpression, EC were plated at a cell density of 60,000 cells/cm^2 and the next day they were infected with a KLF2-GFP adenovirus (EC-KLF2) or a control GFP adenovirus (EC-GFP) at a multiplicity of infection (MOI) of 20 using complete EC media. 24 hr later the media was exchanged for fresh completed media and plated in the transwell or three-dimensional microfluidic device as described below.

4.2.2 Endothelial-smooth muscle transwell co-culture assay

For static endothelial-smooth muscle co-culture studies, endothelial and smooth muscle cells were plated on opposite sides of 24 mm transwell insert (10 μm thick, 1.2 μm pore size) (Corning) (Figure 4.1A). The transwell was prepared for cell culture by coating both surfaces of the membrane with 0.1% gelatin. Smooth muscle cells were plated first for 24 hr in serum-free medium and maintained at 37 °C and 5% CO_2 with 50,000 cells per insert for gene expression studies and 40,000 cells per insert for cell cycle analysis. One day prior to SMC plating, EC were infected with a KLF2 expressing adenovirus (EC-KLF2) or control GFP adenovirus (EC-GFP) at MOI 20 as described above and on the day of SMC replacing the adenovirus containing medium with complete endothelial cell growth. 24 hr after EC media exchange and SMC plating in the transwell, the adenovirus-infected 250,000 EC were plated in co-culture medium (Medium-199 containing 2% FBS, 2 mM L-Glutamine, 100 units/ml penicillin plus 100 μg/ml streptomycin, and 0.03 mg/ml endothelial cell growth supplement) on the opposite side of the transwell insert by inverting the insert and incubating for 1 hr at 37 °C and 5% CO_2. After 1 hr, the transwell was returned to its original position (SMC on the topside of the transwell) and sufficient co-culture medium (~ 3ml total) was placed in and around the transwell to keep the cells hydrated. The co-cultured cells were then maintained for 48 hr at 37 °C and 5% CO_2 (48 – 96 hr post EC infection) before subjecting the SMC to either gene expression or cell cycle analysis.

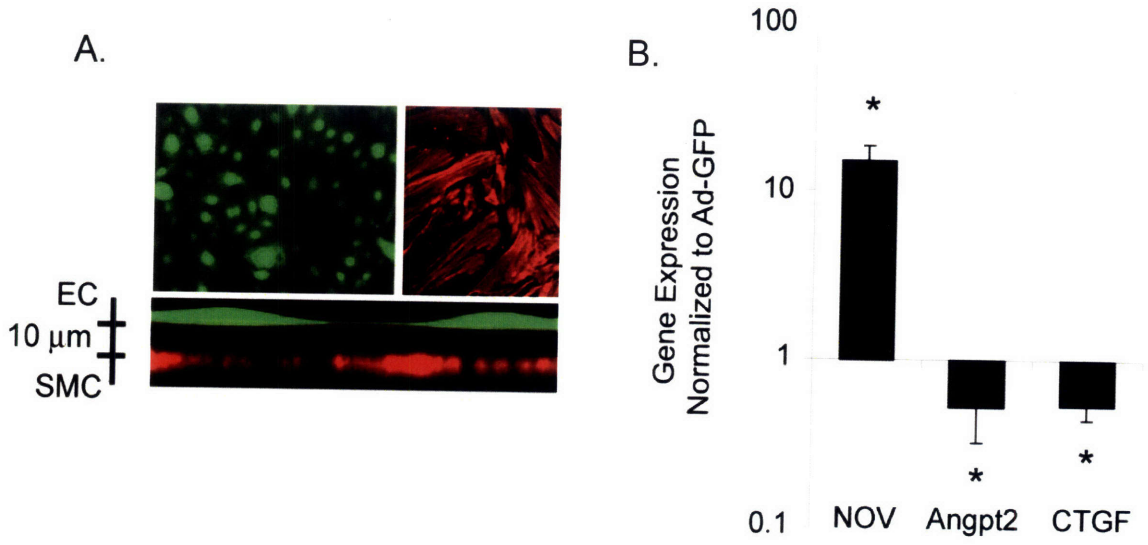

Figure 4.1 EC-SMC transwell co-culture system. B) Adenovirus expression of KLF2 in EC (MOI 20) used for 3D SMC migration assay resulted in downstream EC gene expression patterns, measured by TaqMan real-time PCR, consistent with previously defined KLF2 transcriptional targets and collateral flow-induced gene expression, including NOV, Angpt2, and CTGF. NOV = Nephroblastoma overexpressed; Angpt2 = Angiopoietin 2; CTGF = Connective tissue growth factor. Data represent the mean of 3 independent experiments with the error bars reported as standard error with * $P < 0.05$.

4.2.3 Flow cytometry analysis of cell cycle

The DNA profiles of apoptotic and viable SMC in co-culture with EC expressing KLF2 were assessed by measuring the fluorescent intensity of propidium iodine (PI) for each cell, as described in the Methods section of Chapter 3.

4.2.4 RNA preparation and RT-PCR analysis

Total RNA from adenovirus-infect EC and SMC in co-culture with the genetically modified EC was used for real-time PCR was isolated, purified, quantified and subjected to real-time TaqMan quantitative PCR (Applied Biosystems 7900) as described in the Methods section of Chapter 3.

4.2.5 Microfluidic device fabrication

The microfluidic system was made of PDMS (poly-dimethyl siloxane, Silgard 184, Dow Chemical) using soft lithography with SU-8 patterned wafers as described by others (77). The fabricated devices were autoclaved and then plasma treated for 60 seconds (Harrick) in air, and bonded with sterile #1 circular glass coverslips (VWR) to form closed microfluidic channels. The bonded devices were maintained at 80 °C for 10 minutes to enhance bonding strength and then a 0.1% poly-D lysine (Sigma) coating solution was introduced into the channels and incubated at 37 °C and 5% CO_2 overnight. After coating, the devices were washed twice with sterile water and dried at 80 °C for 24 hours, rendering the channel surfaces hydrophobic. Scaffold material, 0.25% type I collagen (BD Biosciences), was injected into the 3-dimensional device region and incubated for 30 minutes at 37 °C in order to form a 3D hydrogel scaffold for cell invasion. Once the scaffold formed, 0.1% gelatin was then introduced into the microfluidic channels and incubated at 37 °C and 5% CO_2 for 60 minutes to make the channel suitable for cell seeding. The gelatin was then replaced by cell culture medium and allowed to equilibrate for 2 hours at 37 °C at 5% CO_2 before cell seeding.

4.2.6 Three-dimensional migration assay cell seeding and quantification

24 hr after adenovirus infection, EC were seeded via one channel of the 3D-μFD at a density of $2x10^6$ cells/ml in complete Endothelial Growth Medium-2 (EGM-2, Cambrex) and maintained for 24 hr at 37 °C at 5% CO_2. 2 hr prior to SMC seeding, EGM-2 in the microfludic device was exchanged for co-culture medium (Medium-199 containing, 2% FBS, 2 mM L-Glutamine, 100 units/ml penicillin plus 100 μg/ml streptomycin, and 0.03 mg/ml endothelial cell growth

supplement) in order allow the three dimensional region to equilibrate with the co-culture medium. SMC were subsequently labeled with the fluorescent membrane stain PKH26 (Sigma) according to the manufacturer's instructions and seeded in the channel opposing the endothelial channel at a density of 500,000 cells/ml. The EC/SMC co-culture was then maintained at 37 °C and 5% CO_2 for 48 hr before quantification and analysis of SMC migration. For connective tissue growth factor (human recombinant CTGF, Invitrogen) migration studies, the devices were fabricated and the collagen gel was introduced as described above. However, SMC were seeded on the same day as collagen hydrogel injection following 0.1% gelatin coating directly in the co-culture media described above.

SMC 3D invasion for both co-culture and CTGF migration experiments was quantified by staining cell nuclei with DAPI after 48 hr of migration. Briefly, the cells were fixed in 4% paraformaldehyde (PFA) for 60 minutes at room temperature, permeablized with 1% Triton-X for 45 minutes, quenched with PBS containing 5% FBS at room temperature, and DAPI stained overnight at 4 °C. Fluorescent images of cell nuclei and PKH26 stained SMC were then obtained for the entire 3D hydrogel region using an inverted epifluorescent microscope (Nikon Eclipse TE2000-U) and a CCD camera (Sanyo VCB-3524). By merging the two images of different wavelength, nuclei of the pre-labeled SMC could be distinguished from the EC, along with the coordinate position of each SMC within the 3D hydrogel (MetaMorph). The distribution of cell number versus 3D invasion/migration distance and total number of invading cells after 48 hours of co-culture was quantified using this tracking approach.

4.2.7 Statistical analysis

Statistical significance was determined by one-way ANOVA for experiments with more than two

subgroups, while *post hoc* and pairwise comparisons were performed by 2-tailed Student's *t* test for all others (Primer of Biostatistics). *P* values less than 0.05 were considered significant.

4.3 Results

4.3.1 Endothelial KLF2 control of SMC gene expression

An endothelial-smooth muscle cell transwell co-culture system was used to investigate the link between endothelial KLF2 expression and smooth muscle expression of genes identified as regulated by collateral flow in Chapter 3. The transwell system, although a static endothelial cell culture, had the advantage of growing endothelial and smooth muscle cells in close proximity (10 μm) as to permit factors with short bioactive half-lives (i.e. gasses and ecosinoids) to be transported between the cell types while avoiding heterotypic cell contact (Figure 4.1A). Similar to the smooth muscle cell growth chamber that received collateral flow-mediated endothelial conditioned medium, any changes observed in the smooth muscle phenotype could then be attributed to factors secreted by the endothelium.

To test the effect of endothelial KLF2 expression on smooth muscle gene expression, endothelial cells were infected with a KLF2 expression adenovirus (EC-KLF2), control GFP virus (EC-GFP), or no adenovirus (EC). Adenovirus infection of EC with KLF2 lead to the expression pattern of known KLF2 downstream transcriptional targets, including Nephroblastoma overexpressed (NOV), Angiopoietin 2 (Angpt2) and Connective tissue growth factor (CTGF), similar to gene expression levels measured in endothelial cells subjected to

collateral flow (Figure 4.1B). Smooth muscle cells co-cultured with EC (control EC and EC-GFP) in the transwell system were found to display increased expression of Myocardin and alpha-Smooth muscle actin when compared to a no endothelial control (NoEC), as was consistent with the collateral flow experiments (Figure 4.2). Matrix metalloproteinase 3 expression, on the other hand, was found to be modestly reduced in SMC. However, EC expressing KLF2 had comparable effects on SMC gene expression as the EC controls, suggesting that the genes measured are not regulated by KLF2 expression in EC. Kruppel-like factor 4 (KLF4), a smooth muscle transcription factor that negatively regulates smooth muscle expression of contractile proteins and has been reported to be important for vascular remodeling (22), on the other hand, was found to be differentially regulated by control EC and EC expressing KLF2 (Figure 4.2). As an additional measure of EC KLF2 expression on SMC phenotypes, SMC cell cycle progression was also characterized in the EC-SMC transwell co-culture system, but KLF2 expression in EC did not have a significant proliferative effect on the SMC (Figure 4.3). Taken together, endothelial expression of KLF2 does not appear to regulate SMC genes influenced by collateral flow or proliferation, but may regulate other SMC genes that have been shown to be critical in vascular remodeling, such as KLF4.

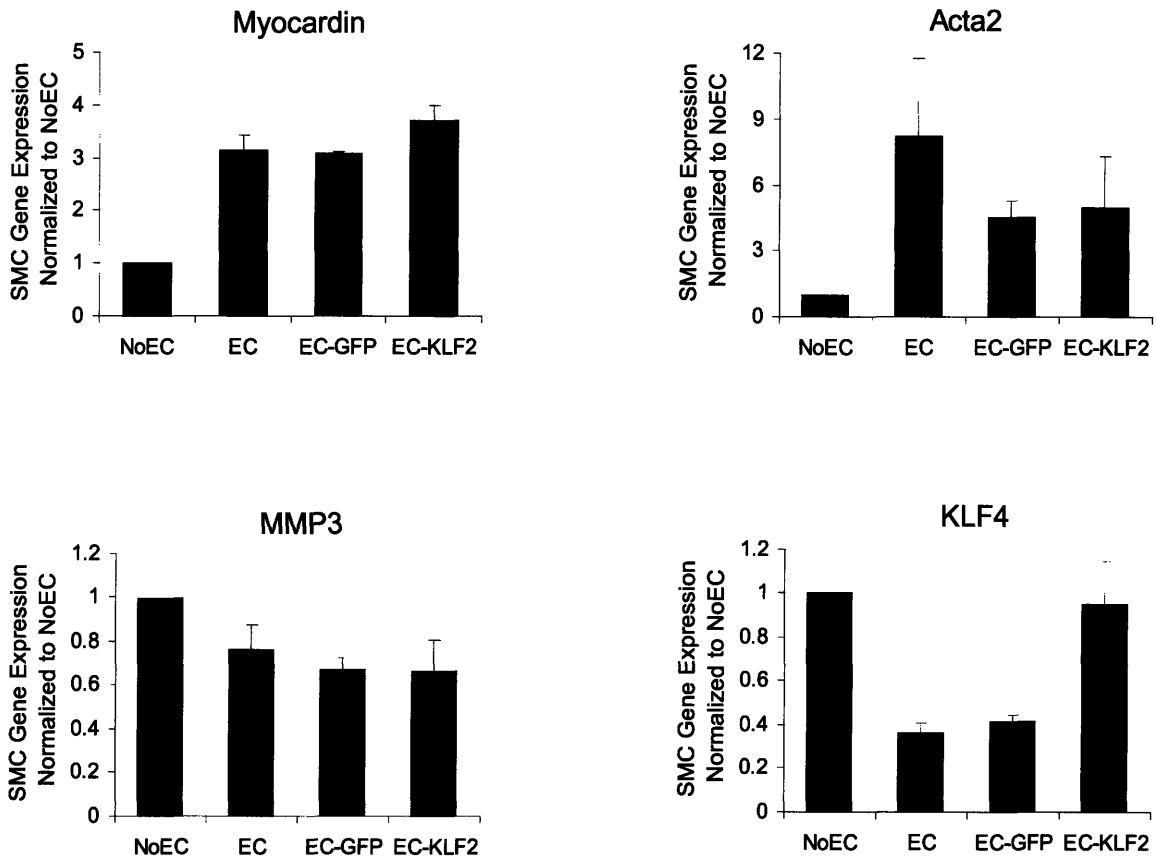

Figure 4.2 SMC were co-cultured in a static transwell system for 48 hr with EC expressing KLF2 and the resulting SMC gene expression was measured using real-time TaqMan PCR. The presence of EC (EC and EC-GFP) was able to induce changes in SMC gene expression for Myocardin, Acta2, MMP3, and KLF4 compared to no endothelial controls (NoEC). However, expression of KLF2 in EC did not alter the expression of these genes in SMC except for KLF4 in which SMC displayed expression levels more comparable to NoEC. NoEC = no endothelial control; EC = non-adenovirus infected EC; EC-GFP = control GFP adenovirus infected EC; EC-KLF2 = KLF2 adenovirus infected EC, Acta2 = alpha Smooth muscle actin; MMP3 = Matrix metalloproteinase 3; KLF4 = Kruppel-like factor 4. Data represents the average of 3 independent experiments with adenovirus infection of MOI 20.

A.

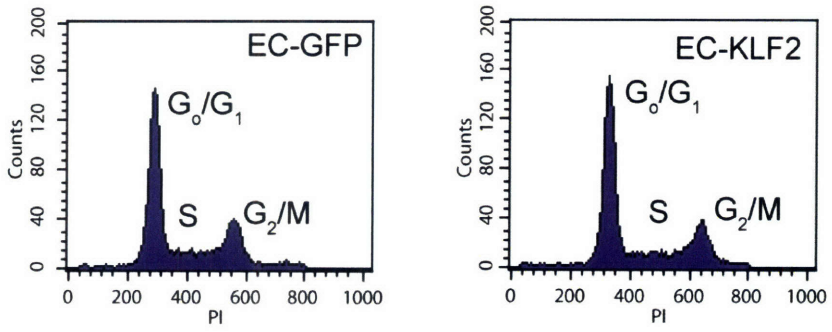

B.

	G_0/G_1	S	G_2/M
NoEC	58.2%	7.8%	30.3%
EC-GFP	65.7%	7.2%	25.4%
EC-KLF2	65.0%	5.9%	27.6%

Figure 4.3 SMC were co-cultured in a static transwell system for 48 hr with EC expressing KLF2 and the resulting effect on SMC proliferation was investigated by DNA labeling with propidium iodine and analyzing for cell cycle using flow cytometry. A) SMC cell cycle data was obtained for a no endothelial control (NoEC) (not shown), EC infected with GFP control adenovirus (EC-GFP), and EC infected with KLF2 adenovirus (EC-KLF2). EC were infected at MOI 20 and 10,000 counts were used for each sample. B) Quantification of the percentage of cells in each phase of the cell cycle revealed that EC KLF2 expression did not result in a significant change in SMC proliferation rates compared to control EC (EC-GFP) or the no endothelial control (NoEC).

4.3.2 Endothelial KLF2 restricts SMC migration

Smooth muscle cell migration is another critical event during embryonic blood vessel formation and adult vascular disease processes such as atherosclerosis, restenosis, and arterial bypass vein grafting in response to changes in the vessel microenvironment (60,76). Accordingly, the ability of endothelial genes evoked by collateral flow to regulate SMC migration, an effect that may have functional implications for adaptive remodeling, was evaluated, with a particular focus on the endothelial expression of KLF2 because multiple collateral flow-mediated endothelial genes

(Table 3.1) have previously been shown to depend on KLF2 (40) and KLF2 has been documented as critical for vascular wall development and function (17,46,47). In order to characterize the effect of endothelial KLF2 expression on SMC migration, a 3-dimensional microfluidic device (3D-μFD) assay was developed to monitor SMC migration in response to EC-generated factors while in co-culture or in response to exogenous factors while in monoculture. The 3D-μFD used here is a PDMS microfabricated system containing two independent flow channels separated by symmetric 1300 μm x 500 μm x 150 μm 3D central regions that were filled with a hydrogel scaffold (type I collagen) (Figure 4.5A-C). Therefore, cells seeded within the individual flow channels can invade the 3D hydrogel and communicate via paracrine signals transported across the hydrogel region. The diffusion transport kinetic in the device was characterized by others using a fluorescent dextran conjugate in which the fluorescent signal can be expressed as a ratio of the input channel concentration, C_o. Using this technique, it was found that a near linear gradient develops within 180 minutes and remains, though to a lesser extent, after 42 hrs (Figure 4.4, where the right side corresponds to C_o).

The effect of EC KLF2 expression on SMC migration was characterized by co-culturing SMC with KLF2 adenovirus-infected EC in opposite channels of the 3D-μFD. SMC migration and invasion into the 3D region was compared between three co-culture conditions: no endothelium (NoEC, Figure 4.5D), GFP control adenovirus (EC-GFP, Figure 4.5E), and KLF2-GFP adenovirus (EC-KLF2, Figure 4.5F). Quantification of 3D SMC migration for the three co-culture conditions revealed that a significantly greater number of SMC invade the 3D region during co-culture with EC-GFP compared to both the no endothelium and EC-KLF2 co-culture conditions, reported as a histogram distribution of cell number versus migration distance (Figure 4.5G) as well as the total number of SMC migrating into the 3D space (Figure 4.5G inset). There

was no significant difference when comparing SMC migration in co-culture with non-infected EC to control GFP-expressing EC (data not shown). Furthermore, as observed with SMC in transwell co-culture with EC, adenovirus-mediated KLF2 expression in EC does not significantly affect SMC proliferation; ruling out the observed effect on SMC migration is an artifact of proliferation (Figure 4.3). These 3D SMC migration results demonstrate that the integrative effect of KLF2 expression in EC acts to reduce SMC migration and provide insight into the molecular program used by endothelial cells to control SMC migration.

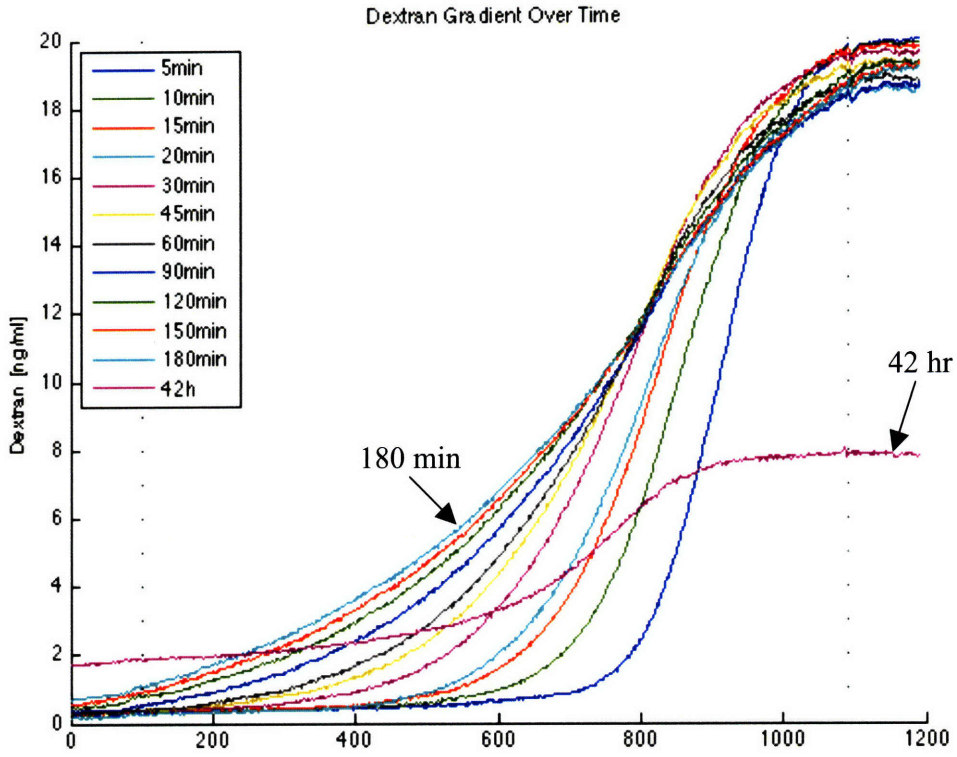

Figure 4.4 Diffusion transport kinetics for dextran in 3D-μFD shows a quasi-stable gradient at early time-points (< 180 minutes) that diminishes in magnitude at later time-points (42 hr) that can be used to estimate the transport of EC-derived paracrine signals or connective tissue growth factor (CTGF) for the SMC migration studies (data and image courtesy of Seok Chung, PhD, MIT Department of Biological Engineering).

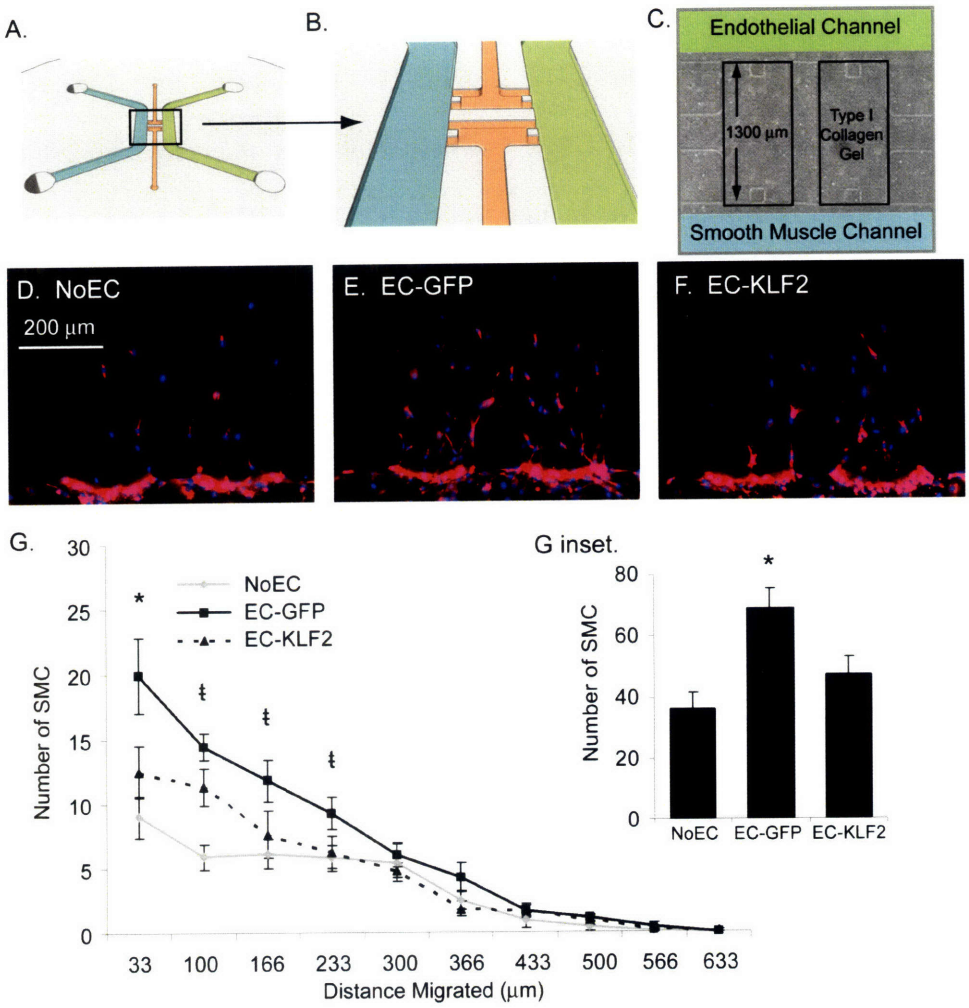

Figure 4.5 EC expressing KLF2 inhibit EC-directed SMC migration. A and B) A 3-dimensional microfluidic bioreactor (3D-μFD) assay was designed in order to investigate SMC migration in response to endothelial-derived factors. The bioreactor has two independent flow channels with each channel separated by a three dimensional region filled with a hydrogel scaffold. C) SMC were cultured in the 3D-μFD in co-culture with EC. A type I collagen scaffold was injected into the three dimensional region and cells were introduced into their respective channels (smooth muscle channel and endothelial channel). Factors generated by EC were transported across the scaffold by passive diffusion. Image shown at 4X magnification and rotated 90° relative to schematics shown in (A) and (B). The cumulative effect of KLF2-dependent EC factors act to inhibit EC-directed 3D SMC migration. 10X fluorescent images of D) no endothelial control (NoEC), E) endothelial cells expressing GFP only (EC-GFP) and F) endothelial cells expressing KLF2 (EC-KLF2). Blue = nuclei (DAPI) and Red = SMC. G) Histogram quantification of the SMC migration distance into the 3D region for the three culture conditions revealed that EC co-culture (EC-GFP) increases SMC migration compared to no endothelial control (NoEC) and that this effect is abolished by KLF2 overexpression in EC (EC-KLF2), as determined by G, inset) the total number of SMC invading the 3D region after 48 hr. Data reported as the mean of 10 (EC-GFP and EC-KLF2) and 9 (NoEC) independent experiments with error bars representing standard error. * $P < 0.05$ across all conditions and ‡ $P < 0.05$ pairwise comparison between NoEC and EC-GFP only.

The inhibited SMC migration in co-culture with EC expression KLF2 was next rescued using connective tissue growth factor (CTGF), an EC gene previously shown to be suppressed by KLF2 under flow (40). Additionally, CTGF has been shown by others to stimulate migration in multiple cell types (78,79) and exist at high levels in atherosclerotic lesions, a focal site of vascular disease associated with increased smooth muscle cell migration (80). Administration of 10 μg/ml CTGF to the channel opposite of SMC in the absence of EC resulted in a significant increase in the total number of SMC migrating into the 3D region after 48 hr compared to control (Figure 4.6A-C). Similarly, CTGF added at the same concentration to the endothelial cell channel in the presence of EC expressing KLF2 restored 3D SMC migration levels to that of SMC co-cultured with control EC (EC-GFP) (Figure 4.6D). These results are consistent with the divergent regulation of CTGF and KLF2 gene expression in EC exposed to collateral shear stress waveforms and indicate that CTGF may constitute a KLF2-dependent EC factor that influences SMC migration. Moreover, these 3D SMC migration results suggest that the gene expression changes evoked by collateral flow during coronary collateralization (e.g. ACC waveform) act to limit SMC migration, which may have important implications for the vessel wall structure during biomechanical regulation of arteriogenesis.

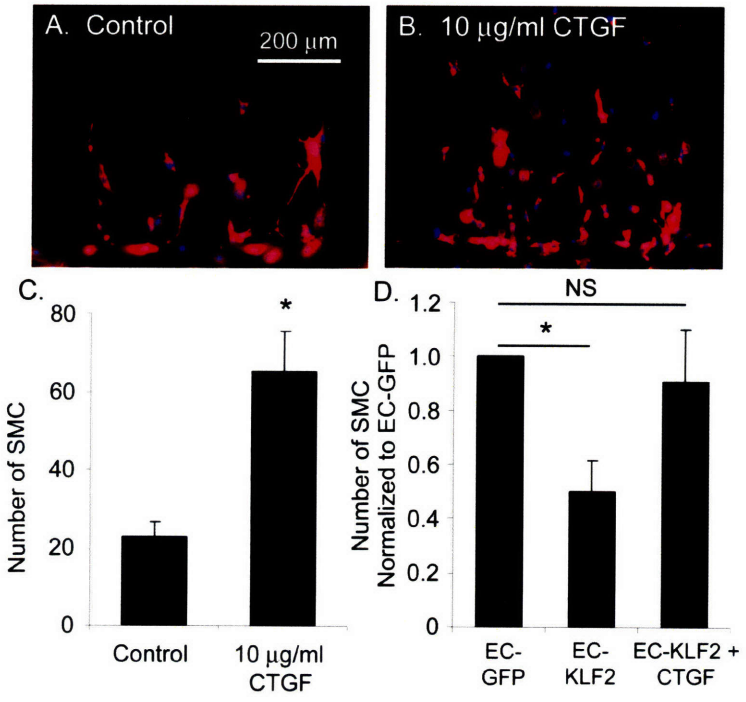

Figure 4.6 Connective tissue growth factor (CTGF) induces SMC migration and rescues the inhibited SMC migration in co-culture with EC expressing KLF2. 10X fluorescent images of A) Control and B) 10 μg/ml CTGF 3D SMC migration. Blue = nuclei (DAPI) and Red = SMC (PKH-26 membrane stain). Quantification of C) the total number of SMC invading the 3D region after 48 hr showed CTGF induced more SMC migration compared to control. D) Addition of 10 μg/ml CTGF to the EC channel in the EC-KLF2 co-culture with SMC returned SMC migration to EC-GFP levels, as shown by normalizing the number of SMC migrating in each test condition to the number migrating in the EC-GFP co-culture condition. Data reported as the mean of 4 (C) or 5 (D) experiments with error bars representing standard error with * $P < 0.05$.

4.4. Discussion

The transcription factor KLF2 emerged from the collateral flow-mediated EC transcriptional profile analysis as a potential key player in regulating an adaptive remodeling endothelial response based on evidence of its flow dependence and necessity to the function of the developing vessel wall. A member of the Kruppel family of zinc finger transcription factors, KLF2 has been shown to be tightly regulated by flow *in vitro* (40,58,81,82) and *in vivo* (40,46), and critical for controlling multiple endothelial phenotypes (40,41,83). A number of other endothelial transcription factors were also regulated by the ACC waveform (see Appendix), but *in vivo* evidence by others indicated that the transcription factor may have a critical role in adaptive remodeling since mice lacking KLF2 display lethal phenotypes of impaired vascular maturation and function. Both *KLF2* -/- mice and endothelial-specific knockout of KLF2 in mice result in embryonic lethality, due either to hemorrhage (17,47) or defects in vascular hemodynamics (46), respectively. Moreover, a recent report by Wu, J et al. documented that the medial layer of vessels of *KLF2*-/- mice is poorly developed, and that SMC of these mice display a patchy morphology with condensed nuclei when compared to wild-type mice (47). Using multiple experimental endothelial-smooth muscle co-culture systems, the effect of endothelial KLF2 expression on smooth muscle gene expression, proliferation, and migration was evaluated based on the premise the KLF2 expression in endothelial cells has the capacity to differentially regulate the release of paracrine signals important for determining smooth muscle molecular and functional phenotypes.

Using 3D SMC migration as a functional SMC read-out, EC KLF2 expression was shown to suppress SMC migration and that this effect can be rescued by the exogenous delivery of

CTGF, an EC secreted factor whose gene expression is reduced by KLF2. The 3D-μFD migration assay as used in these experiments does not allow for cell contact between EC and SMC, indicating that the effect of EC KLF2 expression on SMC migration is partially due to the differential regulation and release of CTGF and other yet to be identified EC factors. The dependence of CTGF secretion from EC on KLF2 expression, however, would need to be verified using an analytical technique such as ELISA, along with the absolute concentration of EC secreted CTGF from the migration assay in order to more definitively characterize the role of CTGF in EC-mediated SMC migration. However, in the absence of obtaining an experimental CTGF measurement, CTGF transport kinetics and the effective concentration presented to SMC was estimated from dextran transport data (Figure 4.4). Assuming a C_o of 10 μg/ml and that CTGF does not interact with the collagen scaffold, interpolation of the dextran transport kinetics estimated the SMC channel concentration of CTGF at early time-points as less than 1% of C_o or 100 ng/ml. Furthermore, after 42 hrs the concentration of CTGF in the SMC channel would be roughly 10% of C_o or 1 μg/ml. Furthermore, since the medium in these experiments was exchanged every 24 hrs it was assumed that CTGF concentrations experienced by SMC were thus less than 1 μg/ml, a concentration similar to what has been measured from the blood of patients with chronic fibrotic diseases (84).

Independent of detailed information regarding the concentration of individual factors secreted by the endothelium, the 3D SMC migration data support the hypothesis that KLF2 has a role in adaptive remodeling by controlling EC-dependent SMC function and suggest that improper regulation of SMC migration may contribute to the vascular wall defects observed in *KLF2*$^{-/-}$ mice. Similar levels of KLF2 expression in EC, however, were not found to alter smooth muscle gene expression or proliferation over a similar period of time, indicating that in the

experimental systems used the effect of KLF2 primarily influences the ability of the endothelium to control smooth muscle migration. Moreover, these data define KLF2 as a potential regulator of EC-induced SMC migration and provide evidence for a transcriptional response by the endothelium to flow that coordinates multiple endothelial genes whose collective expression controls critical interactions with smooth muscle that may promote a stable vessel architecture.

Chapter 5: Conclusions, Future Directions, and Overall Significance

5.1 Conclusions

The molecular mechanisms regulating coronary arteriogenesis, and in particular the cellular events evoked in endothelial cell by hemodynamic forces, remain incompletely defined. Most investigations of arteriogenesis rely on hind limb ischemia animal models while few experimental systems have been implemented in studies of arteriogenesis, possibly due to the high dependence on heterotypic (endothelial, smooth muscle, and inflammatory) cellular interactions during adaptive remodeling processes. To address the open question of how elevated collateral flow acting on the endothelium affects adaptive remodeling cellular events, this Thesis combined numerical simulation, molecular biology, and microenvironmental engineering to demonstrate the shear stress dependence of multiple vascular cell phenotypes critical for the generation of arterial conductance vessels.

Previously undefined numerical simulations of the shear stress waveforms present in coronary vessels with and without an upstream main coronary artery stenosis were first used to

show that collateral flow can differentially regulate both endothelial and smooth muscle cell genes, as evaluated by transcriptional profiling, that have important roles in vessel maturation and stabilization. Kruppel-like factor 2 (KLF2), an endothelial transcription factor, was one such gene found to be upregulated in the endothelium by the arteriogenic coronary collateral waveform. Previous studies have shown KLF2 integrates multiple vasoprotective endothelial phenotypes in response to flow and plays a critical role in vascular development, but little evidence exists linking its expression in the endothelium specifically to coronary collateralization or more broadly to cellular aspects of adaptive remodeling (17,40,47).

The second half of this Thesis focused on the KLF2-dependent endothelial cell interactions with smooth muscle cells. To this end, KLF2 overexpression in static culture was used to interrogate the effect of endothelial KLF2 expression on smooth muscle cell gene expression and migration. Although endothelial KLF2 expression did not alter the expression of smooth muscle cells genes found to be regulated by collateral flow, endothelial KLF2 expression significantly inhibited EC-directed SMC migration and the KLF2-dependent phenotype in smooth muscle cells was rescued in the presence of Connective tissue growth factor (CTGF), an endothelial gene downregulated by collateral flow. Furthermore, although flow acting on the endothelium has previously been observed to affect smooth muscle migration (65), the data documented here provides evidence for a flow-mediated endothelial transcription factor that regulates the functional smooth muscle cell phenotype.

A number of similarities exist between post-natal adaptive arterial remodeling and vascular development. The endothelium in both contexts provides critical signals that direct perivascular or smooth muscle differentiation and function, while blood flow is recognized as a critical determinant of the vessel architecture in the embryo and adult (12,16). Unraveling the

flow-mediated molecular mechanisms important for coronary collateralization in this Thesis drew upon a number of parallels between knowledge gained in the context of embryonic vascular development and adaptive remodeling, yet specific biological processes, including perivascular cell origin, inflammatory cell involvement, and extracellular matrix composition, could also be used to distinguish the two types of vascular formation. In the context of embryonic vascular development, Kuo et al deduced that the vascular defects in KLF2 deficient mice arose from impaired smooth muscle cell recruitment to the vascular wall (17), but the experimental evidence presented here contradicts the interpretation since endothelial KLF2 expression was found to inhibit smooth muscle migration. However, it is possible that KLF2-dependent signals generated by the endothelium influence the migration of perivascular precursor cells differently than adult smooth muscle cells or, as an alternative interpretation, endothelial KLF2 may act to retain perivascular cells within vascular wall while other paracrine signals provide the cues for recruitment (i.e. PDGF-BB). Moreover, smooth muscle cells are present in the arteriole vessel wall during the onset of coronary collateralization, as compared to vascular development in which smooth muscle cells must be recruited to endothelial-only nascent vessels.

Despite the potential differences between embryonic and post-natal KLF2 expression on vascular wall structure and function, KLF2 has been established as critical for embryonic vascular development and the findings of this Thesis suggest that endothelial expression of KLF2 has a critical role in coordinating cellular events that lead to vascular maturation and stabilization during coronary collateralization. Better understandings of both the upstream pathways leading to endothelial KLF2 expression as well as the downstream consequences on adaptive remodeling deserve continued attention. Furthermore, the data documented here sets

the foundation to further define a role of KLF2 in post-natal adaptive remodeling and make advances toward achieving therapeutic arteriogenesis.

5.2 Future directions and therapeutic potential

5.2.1 Role of KLF2 expression in the flow-mediated endothelial regulation of smooth muscle gene expression

An important continuation for investigating the effect of endothelial KLF2 expression on cellular events important for arteriogenesis would be to determine whether endothelial KLF2 is responsible for the changes in smooth muscle gene expression observed following the delivery of collateral flow-mediated endothelial conditioned medium. Preliminary studies to address the open question have focused on different RNA interference strategies for reducing the levels of KLF2 expression in endothelial cells exposed to the arteriogenic coronary collateral (ACC) waveform. To-date the most promising RNA interference approach has been with small interfering RNA (siRNA), although the levels of KLF2 silencing achieved have been suboptimal. Nevertheless, the presence of KLF2 siRNA in EC subjected ACC flow for 24 hr, approximately 72 hr following transient transfection of KLF2 siRNA, yielded a modest 3-fold reduction in KLF2 and delivery conditioned medium from the collateral flow-stimulated EC with control or KLF2 siRNA to smooth muscle cells resulted in no difference in smooth muscle expression of Myocardin nor Matrix metalloproteinase 3 (MMP3) (Appendix A.4). With only a 3-fold reduction in endothelial KLF2 expression, compared to the ideal case of 5-fold or more reduction, these results can be interpreted as there being an insufficient amount of KLF2 silencing in order to see any difference in smooth muscle gene expression or that endothelial

KLF2 expression may not be responsible for the changes in smooth muscle gene expression observed in Chapter 3. Therefore, to clear the uncertainty and gain more insight into the role of KLF2 in arteriogenesis, future experiments should be directed at achieving increased reductions in KLF2 expression under flow followed by the delivery of collateral flow-mediated endothelial conditioned medium to smooth muscle cells.

5.2.2 Defining the *in vivo* effect of KLF2 expression on vascular remodeling

The next step towards realizing the potential of endothelial KLF2 expression in promoting arteriogenesis in the face of arterial occlusion is the generation of animal models that induce vascular remodeling in combination with genetic manipulation of KLF2. Genetic approaches to controlling KLF2 expression *in vivo,* including transient gene delivery and endothelial-specific conditional transgenes, could be used in ischemic hind limb models to identify the effect of endothelial KLF2 expression on arteriogenesis in a native remodeling environment. Based on the results of presented in this Thesis, a rational hypothesis for these animal experiments would be that collateral vessels acquire a more stabilized and mature vascular wall with KLF2 overexpression, while loss of endothelial KLF2 may result in the inability of collateral vessels to fully mature into stable conductance arteries. Moreover, since endothelial dysfunction characteristic of diseases such as diabetes is believed to impair collateral formation (3), KLF2 expression in the endothelium could also be investigated as a target for rescuing the endothelial phenotype in the context of other diseases that affect the vasculature.

Other animal model systems may also prove useful for defining the *in vivo* effect of endothelial KLF2 expression on vascular remodeling. Ideally, an *in vivo* model of coronary collateralization could be used, similar to what has been performed in canines (15), but other

established animal models of vascular remodeling, such as saphenous vein bypass grafting (85) and carotid artery ligation, a low flow model characteristic of pathological remodeling (6), could also be employed. Both of these animal models have demonstrated critical links between hemodynamics and cellular mechanism associated with arterial remodeling, but neither has been used to investigate the specific contributions of endothelial KLF2 expression. Both constitutive overexpression and conditional loss of KLF2 could reveal insights into how the endothelial transcription factor regulates smooth muscle phenotypes and the vessel wall structure and function. For example, carotid ligation leads to phenotypic switching of smooth muscle cells associated with decreased expression of contractile markers and increased migration and proliferation. Since endothelial KLF2 expression was shown here to limit smooth muscle migration, increased KLF2 in the context of low flow-induced vascular remodeling may prevent the elevation in smooth muscle migration and provide partial protection against this pathological remodeling process.

5.2.3 Dissecting the KLF2 regulatory pathway and identifying new pharmacological regulators of KLF2 expression

If KLF2 proves to be an important therapeutic target for promoting coronary collateralization or controlling vascular remodeling processes, it will be important to better understand the signaling pathways that lead to KLF2 expression and identify therapeutic approaches to regulate endothelial KLF2 with high specificity. This could be achieved through gene therapy or the use of chemical compounds. While chemical compounds carry the risk of off-target effects, limits in gene delivery technology pose significant barriers to the short-term applicability of genetically regulating KLF2 expression. The current understanding of flow-mediated signaling events that

control KLF2 expression in endothelial cells is primarily restricted to the MEK5/ERK5/MEF2 axis in which MEK5 (also called BMK1) activation leads to ERK5 phosphorylation and subsequent activation of the KLF2 promoter binding factor and activator MEF2 (40,86). Other documented mechanisms of flow-induced KLF2 expression include PI3kinase-dependent mRNA stabilization (87) and chromatin remodeling of the KLF2 promoter (81). Activation of the MEK5/ERK5/MEF2 cascade is both necessary and sufficient for flow-induced KLF2 transcriptional regulation, as determined by genetic silencing of MEF2, dominant negative forms of MEK5, and ERK5 SUMOylation (40,88). Flow-mediated activation of the MEK5/ERK5/MEF2 axis has also been documented to be critical for inhibiting TNF-induced JNK phosphorylation and the downstream endothelial inflammatory response (86).

Few known regulators of KLF2 expression have been identified in addition to shear stress. Statins, a class of HMG-CoA reductase inhibitors that have several documented pleiotropic effects including the improvement of endothelial dysfunction (89), positively regulate the expression of KLF2 via the MEK5/ERK5/MEF2 signaling cascade and its downstream transcriptional targets in vascular endothelial cells (90), while the inflammatory cytokines tumor necrosis factor alpha (TNF-α) and interleukin 1 (IL-1) (40,87) act as negative biological regulators of KLF2. Overall, activation of the MEK5/ERK5/MEF2 signaling cascade and the resulting increase in KLF2 transcription constitutes a critical molecular indicator of endothelial vasoprotection and the endothelial response to arterial levels of shear stress, which may also include the regulation of adaptive remodeling (Figure 5.1). Recently, a screen for chemical compounds of known biological action was performed in order to identify small molecule regulators of endothelial KLF2 expression. The screen identified novel inducers and suppressors of KLF2 expression, and one of the suppressors, a GSK3 inhibitor, was further validated using a

combination of chemical and genetic approaches (Figure 5.1). A similar approach should also be undertaken to validate the inducers of KLF2 expression, including steroid hormones and resveratrol, since characterization of these compounds and their mechanism of action may ultimately reveal critical regulatory pathways of KLF2 expression. Furthermore, if future efforts in coronary collateralization establish KLF2 as an attractive therapeutic target, the small molecules identified and verified to selectively induce KLF2 expression may ultimately prove integral in achieving therapeutic arteriogenesis

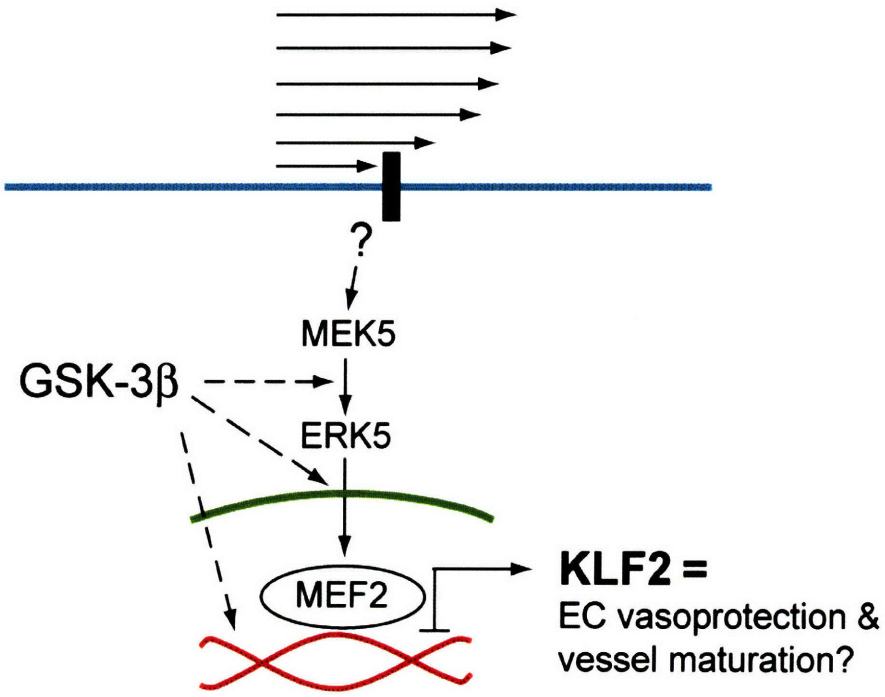

Figure 5.1 The importance of collateral flow-mediated KLF2 expression in the endothelium for directing vessel maturation during *in vivo* arteriogenesis remains to be determined. If KLF2 develops into a target for therapeutic arteriogenesis, or for treating diseases with a vascular defect in vessel maturation such as diabetes and cancer-related solid tumors, the mechano-activated signaling pathway in the endothelium that leads to KLF2 expression should be better defined. Activation of the MEK5/ERK5/MEF2 signaling axis is necessary and sufficient for the cellular response (40). To advance the potential of KLF2 as a therapeutic target for stimulating arteriogenesis, however, both the upstream signaling pathway and the downstream effects on vessel maturation should be further characterized.

5.2.4 Characterizing the role of smooth muscle KLF4 expression on migration

Much of the focus of this Thesis has been on the molecular mechanisms evoked in the endothelium by collateral flow and the resulting effect on smooth muscle cells, while less attention has been dedicated to understanding the smooth muscle-specific molecular mechanisms important for arteriogenesis. Kruppel-like factor 4 (KLF4), a member of the same transcription factor family as KLF2, is an exciting SMC molecular candidate for further investigation since the gene was found to be differentially regulated in SMC co-cultured with endothelial cells expressing different levels of KLF2 (Figure 4.3) and these expression levels of KLF4 correlated inversely with 3D smooth muscle migration (Figure 4.4). A growing body of evidence also exists showing that KLF4 increases in response to growth factor stimulation (i.e. PDGF-BB) and competes with Myocardin to negatively regulate the expression of smooth muscle contractile genes (22). Furthermore, carotid injury animal models demonstrate that loss of KLF4 leads to delayed SMC phenotypic switching, yet overexpression of KLF4 paradoxically produces depressed smooth muscle proliferation where it would be expected to increase proliferation (91). As a follow-up to this Thesis, one logical next step would be to characterize how KLF4 expression in smooth muscle cells influences their migration. Preliminary studies using small interfering RNA (siRNA) to reduce KLF4 expression in SMC, however, did not produce any changes in their baseline migration implying that if KLF4 plays a role in regulating smooth muscle migration it may only be realized in response to specific stimuli, such as paracrine signals from endothelial cells. Nevertheless, a more thorough investigation would be required to

definitively characterize the effect of KLF4 on smooth muscle migration and its importance to arteriogenesis.

5.2.5 Defining stem cell populations that contribute to adaptive remodeling

Another open topic in adaptive remodeling pertains to the precise origin of cells contributing to the process and how these cells interact with resident cells of pre-existing coronary collateral vessel. Both endothelial and smooth muscle cells increase in number during coronary collateralization as the collateral vessel expands, but it is unknown whether this change in cell number results from the proliferation of resident cells or whether it is a result of stem cell recruitment and integration into the vessel. Recent work by Matsuo et al has shown that endothelial progenitor cells purified from peripheral blood can populate growing collateral vessels and improve collateral flow, while mesenchymal stem cells have also been shown to be recruited to the endothelial cells of newly formed vessels (92). Moreover, interactions between endothelial cells and smooth muscle precursors, both through paracrine signals and direct contact, have been demonstrated to lead to the differentiation of mesenchymal stem cells towards a mature smooth muscle cell identity (19,93). Conversely, smooth muscle cells have the capability to control endothelial cell proliferation, migration, and gene expression (16). For the specific adaptive remodeling process of coronary collateralization both resident endothelial and smooth muscle cells are present in the pre-existing collateral arterioles and the experiments designed in this Thesis focused on the interactions between the resident endothelial and smooth muscle cells, but the conclusions may also hold true, at least in part, during interactions with perivascular precursor cells. Recognizing the different cellular interactions in arteriogenesis aids in the interpretation of both the smooth muscle migration and proliferation data documented

here. First, the observation that smooth muscle proliferation does not change with exposure to collateral flow-mediated endothelial conditioned medium or conditioned medium from endothelial cells expressing KLF2 may provide evidence that resident smooth muscle cells do not undergo proliferation changes during collateralization, but rather the increased number of perivascular cells results from the recruitment and/or proliferation of mesenchymal stem cells. Similarly, the inhibitory effect of endothelial KLF2 expression on adult smooth muscle migration may be interpreted as endothelial KLF2-dependent paracrine signals collectively act to retain adult smooth muscle cells at the vascular wall, but the same signals may have different effects on the recruitment and migration of undifferentiated precursor cells. Therefore, defining the contribution of specific resident and recruited cells during arteriogenesis remains a topic that deserves further experimental investigation.

5.3 Overall significance

The impact of this Thesis on the field of arteriogenesis and more broadly its contributions towards understanding the basic mechanisms of adaptive remodeling and endothelial mechano-activation spans the generation of new hemodynamic numerical simulations to defining critical endothelial-dependent events in arteriogenesis. In particular, the endothelial transcriptional profiles evoked by the stimulated collateral vessel shear stress waveforms, as well as its paracrine effect on smooth muscle cells, highlight the role of blood flow in promoting vessel maturation and can be used to guide future studies on the biomechanical regulation of arteriogenesis and blood vessel formation and remodeling. Moreover, the inhibitory effect of endothelial KLF2 expression on smooth muscle migration constitutes the first experimental

evidence in cultured cells linking this endothelial transcription factor to a smooth muscle function critical to maintaining the vessel wall architecture and stability, thereby providing a viable interpretation for the lethal vascular defects observed in KLF2 deficient mice. The challenge now is to further expand our understanding of the molecular and cellular mechanisms regulating coronary collateralization, particularly the transcriptional regulators of critical endothelial and smooth muscle phenotypes, and ultimately translate these basic findings into improved strategies for therapeutic arteriogenesis and other diseases that may benefit from blood vessel stabilization and maturation.

Acknowledgements

First and foremost, I would like to thank my research supervisors, Guillermo García-Cardeña and Roger Kamm. Collectively their mentorship guided me through scientific training in both the engineering and biology disciplines and taught me, by example, to uphold the highest of standards while conducting science and interfacing with members of the scientific community. Furthermore, as mentors, they consistently made my training a top priority and for that I am extraordinarily thankful. I would also like to acknowledge the contributions of my thesis committee members, Richard Lee and Rakesh Jain. These committee members brought invaluable scientific perspectives and experiences to this Thesis and my scientific development benefited greatly from their feedback and our interactions. In addition, crucial technical contributions were made by multiple people, including Yuzhi Zhang and Eric Wang, who helped perform and analyze the microarray data; Vernella Vickerman, Seok Chung, and Iliana Jaatma, who assisted in developing the three dimensional microfluidic smooth muscle migration assay; and Thomas Heldt, who provided expert advice on the hemodynamic numeral simulations. It has been an honor to work along side these talented people, as well as all my past and present lab mates from the García-Cardeña, Kamm, and Gimbrone laboratories, and this body of research would certainly not have evolved into its final form without their contributions. Also, This Thesis would not have been possible without the support, dedication, and motivation provided by friends and family members; and for that I am eternally grateful. Finally, I would like to thank my wife, Christina, for always having the energy to listen to my thoughts and ideas, keeping my goals and priorities in balance, and truly being my number one fan.

References

1. Thom, T., Haase, N., Rosamond, W., Howard, V. J., Rumsfeld, J., Manolio, T., Zheng, Z. J., Flegal, K., O'Donnell, C., Kittner, S., Lloyd-Jones, D., Goff, D. C., Jr., Hong, Y., Adams, R., Friday, G., Furie, K., Gorelick, P., Kissela, B., Marler, J., Meigs, J., Roger, V., Sidney, S., Sorlie, P., Steinberger, J., Wasserthiel-Smoller, S., Wilson, M., and Wolf, P. (2006) *Circulation* **113**(6), e85-151
2. Tayebjee, M. H., Lip, G. Y., and MacFadyen, R. J. (2004) *Qjm* **97**(5), 259-272
3. Roguin, A., Nitecki, S., Rubinstein, I., Nevo, E., Avivi, A., Levy, N. S., Abassi, Z. A., Sabo, E., Lache, O., Frank, M., Hoffman, A., and Levy, A. P. (2003) *Cardiovasc Diabetol* **2**, 18
4. Heil, M., and Schaper, W. (2004) *Circ Res* **95**(5), 449-458
5. Heil, M., and Schaper, W. (2005) *Exs* (94), 181-191
6. Korshunov, V. A., Schwartz, S. M., and Berk, B. C. (2007) *Arterioscler Thromb Vasc Biol* **27**(8), 1722-1728
7. Langille, B. L., and O'Donnell, F. (1986) *Science* **231**(4736), 405-407
8. Rudic, R. D., Shesely, E. G., Maeda, N., Smithies, O., Segal, S. S., and Sessa, W. C. (1998) *J Clin Invest* **101**(4), 731-736
9. Schaper, W., and Scholz, D. (2003) *Arterioscler Thromb Vasc Biol* **23**(7), 1143-1151
10. Rockstroh, J., and Brown, B. G. (2002) *Circulation* **105**(2), 168-173
11. Busse, R., Trogisch, G., and Bassenge, E. (1985) *Basic Res Cardiol* **80**(5), 475-490
12. Jain, R. K. (2003) *Nat Med* **9**(6), 685-693
13. Mecham, R. P., Whitehouse, L. A., Wrenn, D. S., Parks, W. C., Griffin, G. L., Senior, R. M., Crouch, E. C., Stenmark, K. R., and Voelkel, N. F. (1987) *Science* **237**(4813), 423-426
14. Liu, M. W., Roubin, G. S., and King, S. B., 3rd. (1989) *Circulation* **79**(6), 1374-1387
15. Cai, W. J., Kocsis, E., Wu, X., Rodriguez, M., Luo, X., Schaper, W., and Schaper, J. (2004) *Mol Cell Biochem* **264**(1-2), 201-210
16. Carmeliet, P. (2003) *Nat Med* **9**(6), 653-660
17. Kuo, C. T., Veselits, M. L., Barton, K. P., Lu, M. M., Clendenin, C., and Leiden, J. M. (1997) *Genes Dev* **11**(22), 2996-3006
18. Lindahl, P., Hellstrom, M., Kalen, M., and Betsholtz, C. (1998) *Curr Opin Lipidol* **9**(5), 407-411
19. Hirschi, K. K., Rohovsky, S. A., and D'Amore, P. A. (1998) *J Cell Biol* **141**(3), 805-814
20. Lockman, K., Hinson, J. S., Medlin, M. D., Morris, D., Taylor, J. M., and Mack, C. P. (2004) *J Biol Chem* **279**(41), 42422-42430
21. Ma, J., Wang, Q., Fei, T., Han, J. D., and Chen, Y. G. (2006) *Blood*
22. Liu, Y., Sinha, S., McDonald, O. G., Shang, Y., Hoofnagle, M. H., and Owens, G. K. (2005) *J Biol Chem* **280**(10), 9719-9727
23. Suzuki, T., Aizawa, K., Matsumura, T., and Nagai, R. (2005) *Arterioscler Thromb Vasc Biol* **25**(6), 1135-1141
24. Heil, M., Ziegelhoeffer, T., Wagner, S., Fernandez, B., Helisch, A., Martin, S., Tribulova, S., Kuziel, W. A., Bachmann, G., and Schaper, W. (2004) *Circ Res* **94**(5), 671-677

25. Pipp, F., Boehm, S., Cai, W. J., Adili, F., Ziegler, B., Karanovic, G., Ritter, R., Balzer, J., Scheler, C., Schaper, W., and Schmitz-Rixen, T. (2004) *Arterioscler Thromb Vasc Biol* **24**(9), 1664-1668
26. Ferrer, J. M., Lee, H., Chen, J., Pelz, B., Nakamura, F., Kamm, R. D., and Lang, M. J. (2008) *Proc Natl Acad Sci U S A* **105**(27), 9221-9226
27. Robling, A. G., Castillo, A. B., and Turner, C. H. (2006) *Annu Rev Biomed Eng* **8**, 455-498
28. Grodzinsky, A. J., Levenston, M. E., Jin, M., and Frank, E. H. (2000) *Annu Rev Biomed Eng* **2**, 691-713
29. Lammerding, J., Kamm, R. D., and Lee, R. T. (2004) *Ann N Y Acad Sci* **1015**, 53-70
30. Garcia-Cardena, G., and Gimbrone, M. A., Jr. (2006) *Handb Exp Pharmacol* (176 Pt 2), 79-95
31. Chien, S. (2007) *Am J Physiol Heart Circ Physiol* **292**(3), H1209-1224
32. Garcia-Cardena, G., Comander, J., Anderson, K. R., Blackman, B. R., and Gimbrone, M. A., Jr. (2001) *Proc Natl Acad Sci U S A* **98**(8), 4478-4485
33. McCormick, S. M., Eskin, S. G., McIntire, L. V., Teng, C. L., Lu, C. M., Russell, C. G., and Chittur, K. K. (2001) *Proc Natl Acad Sci U S A* **98**(16), 8955-8960
34. Davies, P. F. (1995) *Physiol Rev* **75**(3), 519-560
35. Nauli, S. M., Kawanabe, Y., Kaminski, J. J., Pearce, W. J., Ingber, D. E., and Zhou, J. (2008) *Circulation* **117**(9), 1161-1171
36. Yao, Y., Rabodzey, A., and Dewey, C. F., Jr. (2007) *Am J Physiol Heart Circ Physiol* **293**(2), H1023-1030
37. Dewey, C. F., Jr., Bussolari, S. R., Gimbrone, M. A., Jr., and Davies, P. F. (1981) *J Biomech Eng* **103**(3), 177-185
38. Hsieh, H. J., Li, N. Q., and Frangos, J. A. (1993) *J Cell Physiol* **154**(1), 143-151
39. Dai, G., Kaazempur-Mofrad, M. R., Natarajan, S., Zhang, Y., Vaughn, S., Blackman, B. R., Kamm, R. D., Garcia-Cardena, G., and Gimbrone, M. A., Jr. (2004) *Proc Natl Acad Sci U S A* **101**(41), 14871-14876
40. Parmar, K. M., Larman, H. B., Dai, G., Zhang, Y., Wang, E. T., Moorthy, S. N., Kratz, J. R., Lin, Z., Jain, M. K., Gimbrone, M. A., Jr., and Garcia-Cardena, G. (2006) *J Clin Invest* **116**(1), 49-58
41. Dekker, R. J., Boon, R. A., Rondaij, M. G., Kragt, A., Volger, O. L., Elderkamp, Y. W., Meijers, J. C., Voorberg, J., Pannekoek, H., and Horrevoets, A. J. (2006) *Blood* **107**(11), 4354-4363
42. Rader, D. J., and Daugherty, A. (2008) *Nature* **451**(7181), 904-913
43. Bieker, J. J. (2001) *J Biol Chem* **276**(37), 34355-34358
44. Jiang, J., Chan, Y. S., Loh, Y. H., Cai, J., Tong, G. Q., Lim, C. A., Robson, P., Zhong, S., and Ng, H. H. (2008) *Nat Cell Biol* **10**(3), 353-360
45. Wani, M. A., Means, R. T., Jr., and Lingrel, J. B. (1998) *Transgenic Res* **7**(4), 229-238
46. Lee, J. S., Yu, Q., Shin, J. T., Sebzda, E., Bertozzi, C., Chen, M., Mericko, P., Stadtfeld, M., Zhou, D., Cheng, L., Graf, T., Macrae, C. A., Lepore, J. J., Lo, C. W., and Kahn, M. L. (2006) *Dev Cell* **11**(6), 845-857
47. Wu, J., Bohanan, C. S., Neumann, J. C., and Lingrel, J. B. (2008) *J Biol Chem* **283**(7), 3942-3950
48. Bathe, M., and Kamm, R. D. (1999) *J Biomech Eng* **121**(4), 361-369

49. Draney, M. T., Arko, F. R., Alley, M. T., Markl, M., Herfkens, R. J., Pelc, N. J., Zarins, C. K., and Taylor, C. A. (2004) *Magn Reson Med* **52**(2), 286-295
50. Weinberg, E. J., and Kaazempur Mofrad, M. R. (2007) *Cardiovasc Eng* **7**(4), 140-155
51. Heldt, T., Shim, E. B., Kamm, R. D., and Mark, R. G. (2002) *J Appl Physiol* **92**(3), 1239-1254
52. Schreiner, W., Neumann, F., and Mohl, W. (1990) *J Biomed Eng* **12**(5), 429-443
53. Chaitman, B. R., Bourassa, M. G., Davis, K., Rogers, W. J., Tyras, D. H., Berger, R., Kennedy, J. W., Fisher, L., Judkins, M. P., Mock, M. B., and Killip, T. (1981) *Circulation* **64**(2), 360-367
54. Ku, D. D., and Dai, J. (1997) *J Cardiovasc Pharmacol* **30**(5), 649-657
55. Mees, B., Wagner, S., Ninci, E., Tribulova, S., Martin, S., van Haperen, R., Kostin, S., Heil, M., de Crom, R., and Schaper, W. (2007) *Arterioscler Thromb Vasc Biol* **27**(9), 1926-1933
56. Chen, B. P., Li, Y. S., Zhao, Y., Chen, K. D., Li, S., Lao, J., Yuan, S., Shyy, J. Y., and Chien, S. (2001) *Physiol Genomics* **7**(1), 55-63
57. Dai, G., Vaughn, S., Zhang, Y., Wang, E. T., Garcia-Cardena, G., and Gimbrone, M. A., Jr. (2007) *Circ Res* **101**(7), 723-733
58. Dekker, R. J., van Soest, S., Fontijn, R. D., Salamanca, S., de Groot, P. G., VanBavel, E., Pannekoek, H., and Horrevoets, A. J. (2002) *Blood* **100**(5), 1689-1698
59. Fledderus, J. O., Boon, R. A., Volger, O. L., Hurttila, H., Yla-Herttuala, S., Pannekoek, H., Levonen, A. L., and Horrevoets, A. J. (2008) *Arterioscler Thromb Vasc Biol* **28**(7), 1339-1346
60. Owens, G. K., Kumar, M. S., and Wamhoff, B. R. (2004) *Physiol Rev* **84**(3), 767-801
61. Dardik, A., Yamashita, A., Aziz, F., Asada, H., and Sumpio, B. E. (2005) *J Vasc Surg* **41**(2), 321-331
62. Iivanainen, E., Nelimarkka, L., Elenius, V., Heikkinen, S. M., Junttila, T. T., Sihombing, L., Sundvall, M., Maatta, J. A., Laine, V. J., Yla-Herttuala, S., Higashiyama, S., Alitalo, K., and Elenius, K. (2003) *Faseb J* **17**(12), 1609-1621
63. Hastings, N. E., Simmers, M. B., McDonald, O. G., Wamhoff, B. R., and Blackman, B. R. (2007) *Am J Physiol Cell Physiol* **293**(6), C1824-1833
64. Chiu, J. J., Chen, L. J., Lee, P. L., Lee, C. I., Lo, L. W., Usami, S., and Chien, S. (2003) *Blood* **101**(7), 2667-2674
65. Sakamoto, N., Ohashi, T., and Sato, M. (2006) *Ann Biomed Eng* **34**(3), 408-415
66. Comander, J., Natarajan, S., Gimbrone, M. A., Jr., and Garcia-Cardena, G. (2004) *BMC Genomics* **5**(1), 17
67. Lee, E., Grodzinsky, A. J., Libby, P., Clinton, S. K., Lark, M. W., and Lee, R. T. (1995) *Arterioscler Thromb Vasc Biol* **15**(12), 2284-2289
68. Newby, A. C. (2005) *Physiol Rev* **85**(1), 1-31
69. High, F. A., Lu, M. M., Pear, W. S., Loomes, K. M., Kaestner, K. H., and Epstein, J. A. (2008) *Proc Natl Acad Sci U S A* **105**(6), 1955-1959
70. Jones, N., and Dumont, D. J. (2000) *Cancer Metastasis Rev* **19**(1-2), 13-17
71. Limbourg, A., Ploom, M., Elligsen, D., Sorensen, I., Ziegelhoeffer, T., Gossler, A., Drexler, H., and Limbourg, F. P. (2007) *Circ Res* **100**(3), 363-371
72. Ellis, P. D., Chen, Q., Barker, P. J., Metcalfe, J. C., and Kemp, P. R. (2000) *Arterioscler Thromb Vasc Biol* **20**(8), 1912-1919

73. Lu, H., Xu, X., Zhang, M., Cao, R., Brakenhielm, E., Li, C., Lin, H., Yao, G., Sun, H., Qi, L., Tang, M., Dai, H., Zhang, Y., Su, R., Bi, Y., Zhang, Y., and Cao, Y. (2007) *Proc Natl Acad Sci U S A* **104**(29), 12140-12145
74. Reiss, Y., Droste, J., Heil, M., Tribulova, S., Schmidt, M. H., Schaper, W., Dumont, D. J., and Plate, K. H. (2007) *Circ Res* **101**(1), 88-96
75. Lee, C. W., Stabile, E., Kinnaird, T., Shou, M., Devaney, J. M., Epstein, S. E., and Burnett, M. S. (2004) *J Am Coll Cardiol* **43**(3), 474-482
76. Chatzizisis, Y. S., Coskun, A. U., Jonas, M., Edelman, E. R., Stone, P. H., and Feldman, C. L. (2007) *Curr Opin Cardiol* **22**(6), 552-564
77. Zhao, X., Xia, Y., and Whitesides, G. M. (1997) *J. Mater. Chem.* **7**(7), 1069-1074
78. Cicha, I., Yilmaz, A., Klein, M., Raithel, D., Brigstock, D. R., Daniel, W. G., Goppelt-Struebe, M., and Garlichs, C. D. (2005) *Arterioscler Thromb Vasc Biol* **25**(5), 1008-1013
79. Crean, J. K., Furlong, F., Finlay, D., Mitchell, D., Murphy, M., Conway, B., Brady, H. R., Godson, C., and Martin, F. (2004) *Faseb J* **18**(13), 1541-1543
80. Oemar, B. S., and Luscher, T. F. (1997) *Arterioscler Thromb Vasc Biol* **17**(8), 1483-1489
81. Huddleson, J. P., Ahmad, N., Srinivasan, S., and Lingrel, J. B. (2005) *J Biol Chem* **280**(24), 23371-23379
82. Huddleson, J. P., Srinivasan, S., Ahmad, N., and Lingrel, J. B. (2004) *Biol Chem* **385**(8), 723-729
83. SenBanerjee, S., Lin, Z., Atkins, G. B., Greif, D. M., Rao, R. M., Kumar, A., Feinberg, M. W., Chen, Z., Simon, D. I., Luscinskas, F. W., Michel, T. M., Gimbrone, M. A., Jr., Garcia-Cardena, G., and Jain, M. K. (2004) *J Exp Med* **199**(10), 1305-1315
84. Gressner, A. M., Yagmur, E., Lahme, B., Gressner, O., and Stanzel, S. (2006) *Clin Chem* **52**(9), 1815-1817
85. Kwei, S., Stavrakis, G., Takahas, M., Taylor, G., Folkman, M. J., Gimbrone, M. A., Jr., and Garcia-Cardena, G. (2004) *Am J Pathol* **164**(1), 81-89
86. Berk, B. C. (2008) *Circulation* **117**(8), 1082-1089
87. van Thienen, J. V., Fledderus, J. O., Dekker, R. J., Rohlena, J., van Ijzendoorn, G. A., Kootstra, N. A., Pannekoek, H., and Horrevoets, A. J. (2006) *Cardiovasc Res* **72**(2), 231-240
88. Woo, C. H., Shishido, T., McClain, C., Lim, J. H., Li, J. D., Yang, J., Yan, C., and Abe, J. (2008) *Circ Res* **102**(5), 538-545
89. Davignon, J. (2004) *Circulation* **109**(23 Suppl 1), III39-43
90. Parmar, K. M., Nambudiri, V., Dai, G., Larman, H. B., Gimbrone, M. A., Jr., and Garcia-Cardena, G. (2005) *J Biol Chem* **280**(29), 26714-26719
91. Yoshida, T., Kaestner, K. H., and Owens, G. K. (2008) *Circ Res* **102**(12), 1548-1557
92. Nakano, K., Adachi, Y., Minamino, K., Iwasaki, M., Shigematsu, A., Kiriyama, N., Suzuki, Y., Koike, Y., Mukaide, H., Taniuchi, S., Kobayashi, Y., Kaneko, K., and Ikehara, S. (2006) *Stem Cells* **24**(5), 1274-1279
93. Au, P., Tam, J., Fukumura, D., and Jain, R. K. (2008) *Blood* **111**(9), 4551-4558

Appendices

A.1 Lumped parameter numerical simulation derivation

Variables

P: pressure (mmHg)

Q: flow rate (ml/s)

R: resistance (1 mmHg·s/ml = 1 PRU)

C: compliance (ml/mmHg)

V: compartmental volume (ml)

Subscripts

ao: aorta

ra: right atrium

lv: left ventricle

mca: main coronary artery

col: collateral vessel

st: stenosis in coronary artery

coa: coronary arterioles

coc: coronary capillaries

cov: coronary veins

ext: external (biased) pressure

n: number of collateral vessels

For the model proposed here, the coronary circulation consists of four compartments: the main coronary arteries, arterioles, capillaries, and veins. Forward and reverse pressure-flow rate relationships exist for compartments involving the coronary capillaries and veins due to the pressure-dependent resistances (inversely related to the square of the instantaneous volume) in those compartments. Applying Kirchoff's law (conservation of mass) at each node results in the state form of the node equations written in terms of the flow rates.

Compartmental flow rate equations

(a) Right atrium to coronary arteries

$$Q_{mca} = \frac{P_{ao} - P_{mca}}{R_{mca}} \tag{A1}$$

(b) Coronary arteries to coronary arterioles

$$Q_{st} + nQ_{col} = \frac{P_{mca} - P_{coa}}{R_{st}} + \frac{n(P_{mca} - P_{coa})}{R_{col}} \tag{A2}$$

(c) Coronary arterioles to coronary capillaries

$$Q_{coa} = \begin{cases} \dfrac{P_{coa} - P_{coc}}{R_{coa}} & \text{if } P_{coa} > P_{coc} \\ \dfrac{P_{coa} - P_{coc}}{R_{coa} + 1/V_{coc}^2} & \text{otherwise} \end{cases} \tag{A3}$$

(d) Coronary capillaries to coronary veins

$$Q_{coc} = \begin{cases} \dfrac{P_{coc} - P_{\mathrm{cov}}}{R_{coc} + 1/V_{coc}^2} & \text{if } P_{coc} > P_{\mathrm{cov}} \\ \dfrac{P_{coc} - P_{\mathrm{cov}}}{R_{coc} + 1/V_{\mathrm{cov}}^2} & \text{otherwise} \end{cases} \tag{A4}$$

(e) Coronary veins to right atrium

$$Q_{\mathrm{cov}} = \begin{cases} \dfrac{P_{\mathrm{cov}} - P_{ra}}{R_{\mathrm{cov}} + 1/V_{\mathrm{cov}}^2} & \text{if } P_{\mathrm{cov}} > P_{ra} \\ \dfrac{P_{\mathrm{cov}} - P_{ra}}{R_{\mathrm{cov}}} & \text{otherwise} \end{cases} \tag{A5}$$

Nodal conservation of mass

(a) Main coronary artery node

$$Q_{mca} = Q_{st} + n \cdot Q_{col} + Q'_{mca} \tag{A6}$$

where

$$Q'_{mca} = C_{mca}\frac{dP_{mca}}{dt}$$
$$\therefore \frac{dP_{mca}}{dt} = \frac{Q_{mca} - (Q_{st} + n \cdot Q_{col})}{C_{mca}} \qquad \text{(A7, A8)}$$

(b) Coronary arteriole node

$$Q_{coa} = Q_{st} + n \cdot Q_{col} - Q'_{coa} \qquad \text{(A9)}$$

where

$$Q'_{coa} = C_{coa}\frac{dP_{coa}}{dt}$$
$$\therefore \frac{dP_{coa}}{dt} = \frac{(Q_{st} + n \cdot Q_{col}) - Q_{coa}}{C_{coa}} \qquad \text{(A10, A11)}$$

(c) Coronary capillary node

$$Q_{coc} = Q_{coa} - Q'_{coc} \qquad \text{(A12)}$$

where

$$Q'_{coc} = C_{coc}\frac{dP_{coc}}{dt}$$
$$\therefore \frac{dP_{coc}}{dt} = \frac{Q_{coa} - Q_{coc}}{C_{coc}} \qquad \text{(A13, A14)}$$

(d) Coronary vein node

$$Q_{\text{cov}} = Q_{coc} - Q'_{\text{cov}} \tag{A15}$$

where

$$Q'_{\text{cov}} = C_{\text{cov}} \frac{dP_{\text{cov}}}{dt}$$
$$\therefore \frac{dP_{\text{cov}}}{dt} = \frac{Q_{coc} - Q_{\text{cov}}}{C_{\text{cov}}} \tag{A16, A17}$$

Capillary and venous pressure-dependent volume

(a) Capillary volume

$$V_{coc} = C_{coc}\left(P_{coc} - P_{ext}(t)\right) \tag{A18}$$

(b) Venous volume

$$V_{\text{cov}} = C_{\text{cov}} \cdot P_{\text{cov}} \tag{A19}$$

A.2 Matlab and R code for microarray analysis

A.2.a Lowess Regression, coded in R

```
#working directory is where the data is
#FILE IS 2 COLUMNS WITH RAW INTENSITY VALUES, NO HEADING
thedat<-read.table("PAIREDARRAYSAMPLE.dat",header=FALSE,sep="")
names(thedat)<-c("NCC","ACC")
##thedat$logP<-log(thedat$NCC)+log(thedat$ACC)
attach(thedat)
thedat$logP<-log(NCC)+log(ACC)
thedat$logQ<-log(NCC)-log(ACC)
detach(thedat)
attach(thedat)

#A least squares fit
#thelm<-lm(NCC~ACC)
#summary(thelm)

##theloess1<-
loess(logQ~logP,span=75,degree=2,family="symmetric",na.action=na.omit,model=TRUE)
theloess2<-
loess(logQ~logP,span=.75,degree=2,family="gaussian",na.action=na.omit,model=TRUE)

thedat$newlogQ<-rep(NA,dim(thedat)[1])
thedat[names(theloess2$resid),"newlogQ"]<-theloess2$resid
plot(theloess1$x,theloess1$y)
lines(theloess1$fitted,lwd=2,col="blue")
lines(theloess2$fitted,lwd=2,col="red")

###Checking other bandwidths
for(i in seq(.1,.8,.1)){
                print(i)
        lines(loess(logQ~logP,span=i,degree=2,family="gaussian",na.action=na.omit,model=TR
UE)$fitted,
                col="green")
        }
detach(thedat)
plot(thedat$logP,thedat$newlogQ)
abline(h=0)

write.table(thedat,file="PAIREDARRAYSAMPLE_loess.dat")
```

A.2.b Z-pool statistics coded in Matlab

```
% ************************************************************************
% * Minimum Intensity Z-pool statistics on N=3 microarray data sets
% * Created by Peter J. Mack
% * Garcia-Cardena Lab
% * July, 2007
% ************************************************************************

close all
clear all

% load array 7 columns for N=3 where column 1 is the ABI Probe and remaining 6 are in order
% of experiments (i.e. N=1 condition A; N=1 condition B; N=2 condition A; etc.
% note:  use logged intensity values after Lowess regression

M = load('zpool_val.dat');
[r,c] = size(M);

% calculate the multiplicative factor for minimizing mean square error between arrays
mfn2 = 0;
mfd2 = 0;
mfn3 = 0;
mfd3 = 0;
mfn4 = 0;
mfd4 = 0;
mfn5 = 0;
mfd5 = 0;
mfn6 = 0;
mfd6 = 0;

for i = 1:r
   mfn2 = mfn2 + M(i,2)*M(i,3);
   mfn3 = mfn3 + M(i,2)*M(i,4);
   mfn4 = mfn4 + M(i,2)*M(i,5);
   mfn5 = mfn5 + M(i,2)*M(i,6);
   mfn6 = mfn6 + M(i,2)*M(i,7);

   mfd2 = mfd2 + M(i,3)*M(i,3);
   mfd3 = mfd3 + M(i,4)*M(i,4);
   mfd4 = mfd4 + M(i,5)*M(i,5);
   mfd5 = mfd5 + M(i,6)*M(i,6);
```

```
   mfd6 = mfd6 + M(i,7)*M(i,7);

end
mf2 = mfn2./mfd2;
mf3 = mfn3./mfd3;
mf4 = mfn4./mfd4;
mf5 = mfn5./mfd5;
mf6 = mfn6./mfd6;

M(:,3) = mf2.*M(:,3);
M(:,4) = mf3.*M(:,4);
M(:,5) = mf4.*M(:,5);
M(:,6) = mf5.*M(:,6);
M(:,7) = mf6.*M(:,7);

% calculate the minimum intensity and average ratio across both array spots (X = NCC, Y =
ACC)
M1 = M(:,3)-M(:,2);  % calculates the log(ACC/NCC)
M2 = M(:,5)-M(:,4);
M3 = M(:,7)-M(:,6);

scatdat = M(:,2:7);
save scatterdat.dat scatdat -ascii

for i = 1:r
   Imin(i) = min(M(i,(2:7)));
   Iave(i) = mean(M(i,(2:7)));
   Mave(i) = mean([M1(i),M2(i),M3(i)]);
end
Imin = Imin';
Iave = Iave';
Mave = Mave';

M(:,8) = Imin;
M(:,9) = M1;
M(:,10) = M2;
M(:,11) = M3;
M(:,12) = Mave;

% calculate the variance for each condition
for i = 1:r
   Var(i) = var(M(i,(9:11)));
end
Var = Var';
M(:,13) = Var;
```

```
Msort = sortrows(M,8);
Var_sort = Msort(:,13);

% pool the variances +/- 250 spots
for i = 1:r
   if i <= 250
      Vave(i) = mean(Var_sort(1:(i+250)));
   elseif i >= 251 & i <= (r-250)
      Vave(i) = mean(Var_sort((i-250):(i+250)));
   else
      Vave(i) = mean(Var_sort((i-250):r));
   end
end
Vave = Vave';
Msort(:,14) = Vave;

% calculate Z statistic and p-value
for i = 1:r
   Z(i) = Msort(i,12)/sqrt(Msort(i,14)/3);
   z = abs(Z(i));
   p(i) = 1-2*quad('exp(-0.5*(x.^2))/(sqrt(2*pi))',0,abs(z));
   RQ1 = exp(Msort(i,9));
   RQ2 = exp(Msort(i,10));
   RQ3 = exp(Msort(i,11));
   RQ(i) = mean([RQ1,RQ2,RQ3]);
end

RQ = RQ';
pout = zeros(r,3);
pout(:,1) = Msort(:,1);   % Probe ID
pout(:,2) = RQ;       % ACC/NCC (with multiplicative factor if used)
p = p';
pout(:,3) = abs(p);   % P value

% Define P value cut-off and export data file
a = 0;
for i=1:r
   if pout(i,3) <= 0.01
      a = a+1;
      psort(a,1) = pout(i,1);
      psort(a,2) = pout(i,2);
      psort(a,3) = pout(i,3);
   end
end

% save pvalue.dat pout -ascii
```

```
save pvalue_sort.dat psort -ascii

scatdat = M(:,1:7);
save scatterdat.dat scatdat -ascii
```

A.3 Collateral flow-mediated endothelial transcription and secreted factors

Transcription Factors up-regulated by the ACC Waveform

RefSeq	Gene Name; Symbol	ACC/NCC	P-value
NM_016270.1	Kruppel-like factor 2 (lung);KLF2	4.558	5.77E-08
NM_002165.2	inhibitor of DNA binding 1;ID1	3.996	8.72E-07
NM_001451.1	forkhead box F1;FOXF1	3.785	4.65E-05
NM_024310.2	pleckstrin homology domain containing, family F member 1;PLEKHF1	3.431	1.12E-04
AF150628.1	Kruppel-like factor 13;KLF13	3.362	4.52E-05
NM_004089.2	TSC22 domain family, member 3;TSC22D3	3.345	2.65E-04
NM_207336.1	zinc finger protein 467;ZNF467	2.995	7.24E-05
NM_001290.1	LIM domain binding 2;LDB2	2.862	6.01E-07
NM_003670.1	basic helix-loop-helix domain containing, class B, 2;BHLHB2	2.203	7.30E-05
NM_002166.4	inhibitor of DNA binding 2;ID2	2.121	1.57E-06
NM_005655.1	Kruppel-like factor 10;KLF10	2.037	5.31E-05
NM_153219.2	zinc finger protein 524;ZNF524	1.964	4.45E-04
NM_201443.1	TEA domain family member 4;TEAD4	1.916	2.58E-05
NM_005574.2	LIM domain only 2 (rhombotin-like 1);LMO2	1.871	5.68E-05
NM_004735.1	leucine rich repeat (in FLII) interacting protein 1;LRRFIP1	1.844	3.18E-05
NM_004688.1	N-myc (and STAT) interactor;NMI	1.815	2.63E-04
NM_006521.3	transcription factor binding to IGHM enhancer 3;TFE3	1.724	4.88E-04
AK094201.1	zinc finger and BTB domain containing 38;ZBTB38	1.697	7.13E-04

Secreted Factors up-regulated by the ACC Waveform

RefSeq	Gene Name; Symbol	ACC/NCC	P-value
NM_002514.2	nephroblastoma overexpressed gene;NOV	26.547	8.06E-07
NM_182511.2	cerebellin 2 precursor;CBLN2	8.466	7.14E-08
NM_198966.1	parathyroid hormone-like hormone;PTHLH	5.606	8.44E-07
NM_194435.1	vasoactive intestinal peptide;VIP	4.739	1.58E-04
NM_003862.1	fibroblast growth factor 18;FGF18	4.247	4.34E-07
NM_001998.1	fibulin 2;FBLN2	4.032	5.67E-08
NM_002308.2	lectin, galactoside-binding, soluble, 9 (galectin 9);LGALS9	2.791	9.13E-04
NM_020634.1	growth differentiation factor 3;GDF3	2.729	4.87E-07
NM_005429.2	vascular endothelial growth factor C;VEGFC	2.724	5.81E-08
NM_000214.1	jagged 1 (Alagille syndrome);JAG1	2.290	1.93E-08
NM_002006.3	fibroblast growth factor 2 (basic);FGF2	2.272	6.10E-05
NM_000138.2	fibrillin 1;FBN1	2.105	7.41E-08
NM_003087.1	synuclein, gamma (breast cancer-specific protein 1);SNCG	1.891	4.95E-05
NM_004864.1	growth differentiation factor 15;GDF15	1.752	3.49E-05
NM_014624.2	S100 calcium binding protein A6 (calcyclin);S100A6	1.749	3.03E-08
NM_000611.4	CD59 molecule, complement regulatory protein;CD59	1.581	1.75E-06

Transcription Factors down-regulated by the ACC waveform

RefSeq	Gene Name; Symbol	ACC/NCC	P-value
NM_006101.1	kinetochore associated 2;KNTC2	-4.607	1.92E-05
NM_152278.1	transcription elongation factor A (SII)-like 7;TCEAL7	-3.743	3.18E-05
NM_013282.2	ubiquitin-like, containing PHD and RING finger domains, 1;UHRF1	-3.246	7.15E-07
NM_003199.1	transcription factor 4;TCF4	-2.915	1.21E-06
NM_005842.2	sprouty homolog 2 (Drosophila);SPRY2	-2.693	7.80E-08
NM_012081.3	elongation factor, RNA polymerase II, 2;ELL2	-2.393	2.21E-04
NM_003107.2	SRY (sex determining region Y)-box 4;SOX4	-2.362	8.29E-08
NM_005900.1	SMAD, mothers against DPP homolog 1 (Drosophila);SMAD1	-2.305	5.08E-08
NM_004219.2	pituitary tumor-transforming 1;PTTG1	-2.271	7.27E-08
NM_002015.2	forkhead box O1A (rhabdomyosarcoma);FOXO1A	-2.130	3.46E-07
NM_201557.1	four and a half LIM domains 2;FHL2	-1.977	7.54E-08
NM_006079.2	Cbp/p300-interacting transactivator 2;CITED2	-1.957	2.96E-05
NM_004657.3	serum deprivation response (phosphatidylserine binding protein);SDPR	-1.882	9.17E-07
NM_001300.3	Kruppel-like factor 6;KLF6	-1.804	1.81E-04
NM_004289.5	nuclear factor (erythroid-derived 2)-like 3;NFE2L3	-1.755	1.91E-04
NM_032999.1	general transcription factor II, i;GTF2I	-1.686	1.13E-04
NM_015461.1	zinc finger protein 521;ZNF521	-1.576	7.24E-04
BX648300.1	cAMP responsive element binding protein 3-like 2;CREB3L2	-1.561	9.01E-04
NM_005230.2	ELK3, ETS-domain protein (SRF accessory protein 2);ELK3	-1.555	7.35E-04
NM_000964.1	anaplastic lymphoma kinase (Ki-1);ALK	-1.524	3.06E-04
NM_000964.1	retinoic acid receptor, alpha;RARA	-1.524	3.06E-04
NM_000964.1	nucleophosmin (nucleolar phosphoprotein B23, numatrin);NPM1	-1.524	3.06E-04

Secreted Factors down-regulated by the ACC waveform

RefSeq	Gene Name; Symbol	ACC/NCC	P-value
NM_001147.1	angiopoietin 2;ANGPT2	-9.966	7.07E-07
NM_002982.2	chemokine (C-C motif) ligand 2;CCL2	-4.639	1.60E-07
NM_005127.2	C-type lectin domain family 2, member B;CLEC2B	-3.827	2.18E-07
NM_006329.2	fibulin 5;FBLN5	-3.666	4.21E-06
NM_000584.2	interleukin 8;IL8	-3.547	1.29E-06
NM_003246.2	thrombospondin 1;THBS1	-3.504	1.24E-07
NM_001955.2	endothelin 1;EDN1	-3.024	1.75E-06
NM_001511.1	chemokine (C-X-C motif) ligand 1;CXCL1	-2.867	7.30E-08
NM_004167.3	chemokine (C-C motif) ligand 14;CCL14	-2.846	7.40E-08
NM_004167.3	chemokine (C-C motif) ligand 15;CCL15	-2.846	7.40E-08
NM_005842.2	sprouty homolog 2 (Drosophila);SPRY2	-2.693	7.80E-08
NM_001901.1	connective tissue growth factor;CTGF	-2.676	4.75E-07
NM_018894.1	EGF-containing fibulin-like extracellular matrix protein 1;EFEMP1	-2.545	1.78E-06
NM_001200.1	bone morphogenetic protein 2;BMP2	-2.544	5.27E-08
NM_006080.1	sema domain, immunoglobulin domain (Ig), (semaphorin) 3A;SEMA3A	-2.511	4.20E-04
NM_130851.1	bone morphogenetic protein 4;BMP4	-2.505	7.09E-08
NM_001175.1	Rho GDP dissociation inhibitor (GDI) beta;ARHGDIB	-2.398	7.76E-08
NM_007036.2	endothelial cell-specific molecule 1;ESM1	-2.373	4.56E-08
NM_001124.1	adrenomedullin;ADM	-2.255	1.69E-05
NM_001554.3	cysteine-rich, angiogenic inducer, 61;CYR61	-2.216	6.52E-07
NM_003239.1	transforming growth factor, beta 2;TGFB2	-2.152	2.20E-07
NM_004124.2	glia maturation factor, beta;GMFB	-2.150	1.82E-05
NM_002356.4	myristoylated alanine-rich protein kinase C substrate;MARCKS	-2.129	1.00E-08
NM_182790.1	pre-B-cell colony enhancing factor 1;PBEF1	-2.108	1.43E-05
NM_000900.1	matrix Gla protein;MGP	-1.868	7.58E-08
NM_005723.2	tetraspanin 5;TSPAN5	-1.764	6.81E-04
NM_001343.1	disabled homolog 2;DAB2	-1.690	6.70E-05
NM_022475.1	hedgehog interacting protein;HHIP	-1.670	3.50E-04
NM_175060.1	C-type lectin domain family 14, member A;CLEC14A	-1.652	1.63E-04
NM_005230.2	ELK3, ETS-domain protein (SRF accessory protein 2);ELK3	-1.555	7.35E-04

A.4 Effect of KLF2 silencing in EC on cellular events critical for arteriogenesis

Preliminary results

Silencing KLF2 expression in endothelial cells subjected to the arteriogenic coronary collateral (ACC) waveform, delivering the resulting endothelial conditioned medium to smooth muscle cells, and assessing the smooth muscle cells for changes in gene expression, namely Myocardin and Matrix metalloproteinase 3, would provide mechanistic insight into the molecular mechanisms regulating endothelial control over smooth muscle gene expression. Preliminary experiments, achieving a 3-fold (Figure A.1.A), siRNA-mediated reduction in ACC flow-induced endothelial KLF2 expression, however, did not result in any significant changes in smooth muscle gene expression (Figure A.1.B). These results may reflect an insufficient silencing of endothelial KLF2 expression or that KLF2-depended endothelial secreted factors not regulate the expression of these smooth muscle genes.

Transient transfection of HUVEC with siRNA

Transient transfection of HUVEC with siRNA duplexes against human KLF2 (Sense: 5'-ACCAAGAGUUCGCAUCUGAtt-3', Antisense: 3'-UCAGAUGCGAACUCUUGGUgt-5') was performed by plating EC at a density of 43,000 cells/cm^2 in the full dynamic flow system shear plate 16 hours prior to transfection in complete growth medium. At the time of transfection with siRNA, the cells had reached 85-95% confluence. Individual siRNAs were mixed with Oligofectamine (KLF2 siRNA or negative control siRNA, each at a final concentration of 20 nM) and Opti-MEM (Invitrogen) to a final volume of 2 ml and allowed to incubate at room temperature for 15 minutes to allow the lipid-siRNA complexes to form. Prior to the incubation,

80 µl of Oligofectamine had been pre-incubated with 920 µl of Opti-MEM for 5 minutes at room temperature. The HUVEC were washed once and 8 ml of Opti-MEM was added. Once the lipid-siRNA complexes had formed, the 2 ml mixture was added to the EC in dropwise and the plate was gentle rocked before incubating at 37 °C and 5% CO_2. 6 hr later, 5 ml of complete EC growth media without antibiotics was added to the plate and 20 hr later the media was exchanged for complete EC media. 24 hr later, the ACC collateral waveform was initiated in the dynamic flow system and endothelial conditioned medium was delivered to cultured smooth muscle cells as described in the Methods section of Chapter 3. After 24 hr exposure to flow, gene expression in both the EC and SMC was assessed as described in the Methods section of Chapter 3.

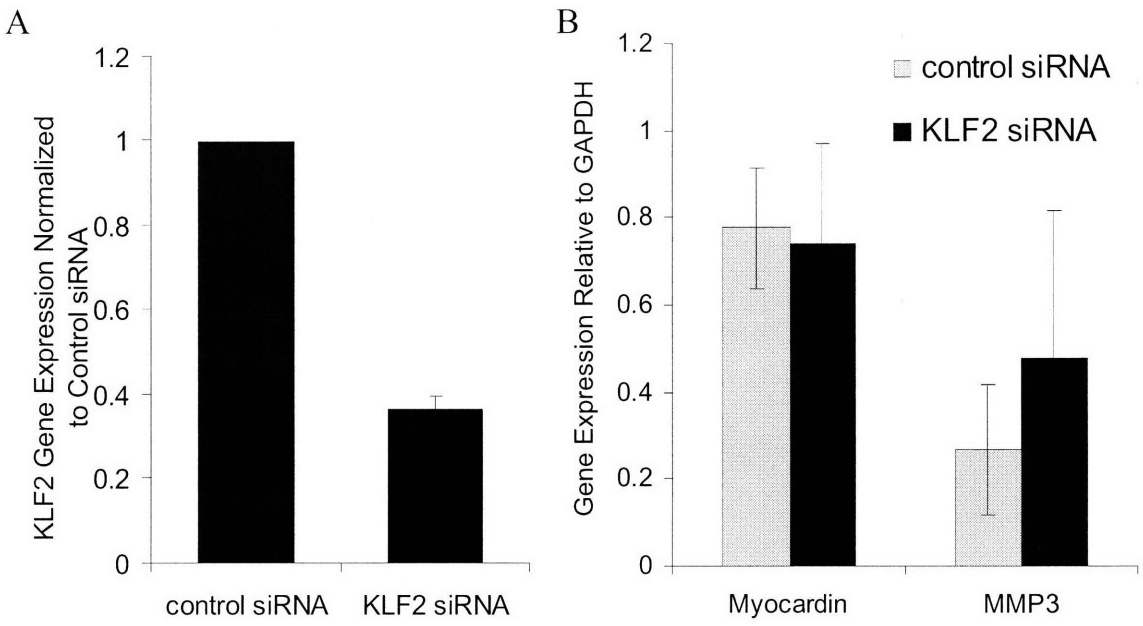

Figure A.1 A) Small interfereing RNA (siRNA) was used to reduce KLF2 expression by 3-fold in endothelial cells exposed to the arteriogenic coronary collateral (ACC) waveform, as compared to control siRNA. B) Delivery of conditioned medium from the endothelial flow experiments did not result in any significant changes in smooth muscle Myocardin or Matrix metalloproteinase 3 expression. Data represent the average of 2 independent experiments +/- standard deviation.